Regioselective Complexation of Unprotected Carbohydrates by Platinum(II): Synthesis, Structure, Complexation Equilibria, and Hydrogen-Bonding in Carbonate-Derived Bis(phosphine)platinum(II) Diolate and Alditolate Complexes

Mark A. Andrews,* Eric J. Voss, George L. Gould, Wim T. Klooster, and Thomas F. Koetzle

Contribution from the Department of Chemistry, Brookhaven National Laboratory, P.O. Box 5000, Upton, New York 11973-5000

*Received April 28, 1993**

Abstract: Treatment of bis(phosphine)platinum(II) carbonate complexes (LL)Pt(CO_3) (e.g., LL = 1,3-bis(diphenylphosphino)propane) with vicinal diols (i.e., $HOCR^1R^2CR^3R^4OH$) gives equilibrium conversion to the corresponding diolate complexes (LL)Pt($OCR^1R^2CR^3R^4O$), which are readily isolated in good yield. From competition experiments, relative diol complexation constants were determined as a function of both the diol and the phosphine substituents and found to span a range of over 10^4. Corresponding triolate and alditolate complexes were similarly prepared, for which very distinct equilibrium isomeric regioselectivities are observed, favoring complexation of *γ,δ-threo* diols. An X-ray structure of (dppp)Pt(D-mannitolate) shows that the mannitol is bonded to the platinum as its dianion via the oxygens on C3 and C4 to form a 2,5-dioxaplatinacyclopentane chelate ring and that three different strong intramolecular hydrogen-bonding interactions are present between the hydroxyl hydrogens and the metallacycle oxygens (O···O (av) = 2.65(2) Å), forming five-, six-, and seven-membered rings. Crystal data for $PtP_2O_6C_{33}H_{38}\cdot CH_2Cl_2$: $P2_12_12_1$, Z = 4, $T \approx 20$ °C, a = 11.225(2) Å, b = 15.875(3) Å, c = 19.964(4) Å, $R(F_o)$ = 0.058, $R_w(F_o)$ = 0.062.

Introduction

The success of a catalytic reaction is dependent upon the quality of the catalyst–substrate match. The high selectivity of homogeneous organo-transition-metal catalysts[1] should be an ideal complement to the functional complexity of native carbohydrate substrates, but this hypothesis is virtually unexplored.[2-7] Anticipated benefits of such studies range from new carbohydrate synthetic methodologies, less dependent upon temporary protecting groups,[8] to alternative approaches to the utilization of our renewable biomass resources.[9] An understanding of stoichiometric metal–carbohydrate interactions is a fundamental prerequisite to achieving these goals. While the interactions of simple metal ions with carbohydrates have been extensively investigated,[10-12] organo-transition-metal complexes of unprotected carbohydrates are essentially unknown.[13-16] Unfortunately, the former cannot be relied upon as good models for the latter, as the two types of complexes would be expected to exhibit very different coordination modes and reactivity patterns. Since the most characteristic functionality of carbohydrates is the diol unit, we looked to studies of organo-transition-metal diolate complexes as more suitable models. Even this class of compounds has received little focused attention, despite its relevance to alkene oxidation.[13,17-21]

We present here an overview of our emerging, multifaceted investigation of the complexation of diols, both simple and complex, to the prototypical metal fragment bis(phosphine)platinum(II). Key findings include (1) the development of a general new synthetic method for the preparation of diolate complexes based on the reaction of metal carbonates with diols, (2) the discovery that the kinetics and thermodynamics of this reaction are suitable for determining relative stability constants for diol complexation, (3) the isolation and characterization of the first organo-transition-metal complexes of nontrivial, unprotected carbohydrates, (4) the observation of several types of high complexation regioselectivity, and (5) the demonstration of

* Abstract published in *Advance ACS Abstracts*, June 1, 1994.

(1) Parshall, G. W.; Ittel, S. D. *Homogeneous Catalysis: The Applications and Chemistry of Catalysis by Soluble Transition Metal Complexes*, 2nd ed.; Wiley: New York, 1992.

(2) Andrews, M. A.; Klaeren, S. A. *J. Am. Chem. Soc.* **1989**, *111*, 4131–4133.

(3) Massoui, M.; Beaupere, D.; Goethals, G.; Uzan, R. *J. Mol. Catal.* **1985**, *29*, 7–12.

(4) Pillai, S. M.; Vancheesan, S.; Rajaram, J.; Kuriacose, J. C. *J. Mol. Catal.* **1982**, *16*, 349–358.

(5) Rajagopal, S.; Vancheesan, S.; Rajaram, J.; Kuriacose, J. C. *J. Mol. Catal.* **1993**, *81*, 185–194.

(6) Kruse, W. M.; Wright, L. W. *Carbohydr. Res.* **1978**, *64*, 293–296.

(7) Kruse, W. M. U.S. Patent 3,935,284, Jan 1976.

(8) Andrews, M. A.; Gould, G. L.; Klaeren, S. A. *J. Org. Chem.* **1989**, *54*, 5257–5264.

(9) Andrews, M. A.; Klaeren, S. A.; Gould, G. L. In *Carbohydrates as Organic Raw Materials II*; Descotes, G., Ed.; VCH: New York, 1993; pp 3–25.

(10) Whitfield, D. M.; Stojkovski, S.; Sarkar, B. *Coord. Chem. Rev.* **1993**, *122*, 171–225.

(11) Angyal, S. J. *Adv. Carbohydr. Chem. Biochem.* **1989**, *47*, 1–43.

(12) Yano, S. *Coord. Chem. Rev.* **1988**, *92*, 113–156.

(13) A bis(phosphine)platinum(II) glycerolate complex has been reported (Appelt, A.; Willis, A. C.; Wild, S. B. *J. Chem. Soc., Chem. Commun.* **1988**, 938–940), but there are minimal regioselectivity considerations involved in the complexation of this simple C_3 protoalditol.

(14) In keeping with long-standing tradition, we include low-valent metal phosphine complexes in the category of organo-transition-metal complexes (see, for example, the Instructions to Authors in *Organometallics*).

(15) A computerized Chemical Abstracts Service substructure search was made for all transition-metal complexes having a metal–carbon or metal–phosphorus bond and a 2,5-dioxametallacyclopentane fragment with at least one α-CHOH substituent.

(16) There are a number of organometallic studies of protected sugars (see, for example: Daves, G. D., Jr. *Acc. Chem. Res.* **1990**, *23*, 201–206. DeShong, P.; Slough, G. A.; Elango, V.; Trainor, G. L. *J. Am. Chem. Soc.* **1985**, *107*, 7788–7790. Descotes, G.; Sinou, D.; Praly, J.-P. *Carbohydr. Res.* **1980**, *78*, 25–32), but here regioselectivity issues are greatly diminished compared to those for native carbohydrates.

(17) Bryndza, H. E.; Calabrese, J. C.; Marsi, M.; Roe, D. C.; Tam, W.; Bercaw, J. E. *J. Am. Chem. Soc.* **1986**, *108*, 4805–4813.

(18) Gable, K. P.; Phan, T. N. *J. Am. Chem. Soc.* **1994**, *116*, 833–839.

(19) Herrmann, W. A.; Marz, D.; Herdtweck, E.; Schäfer, A.; Wagner, W.; Kneuper, H.-J. *Angew. Chem., Int. Ed. Engl.* **1987**, *26*, 462–464.

(20) Herrmann, W. A.; Watzlowik, P.; Kiprof, P. *Chem. Ber.* **1991**, *124*, 1101–106.

(21) Andrews, M. A.; Gould, G. L. *Organometallics* **1991**, *10*, 387–389.

0002-7863/94/1516-5730$04.50/0

Table 1. Yields and ^{31}P NMR Data for (dppp)Pt(diolate) Complexes[a]

		yield, %	δP_A (J_{PtP_A})	δP_B (J_{PtP_B})
		Diols		
1,2-ethanediol		78	−8.1 (3154)	
1,2-propanediol		75	−8.3 (3124)	−9.3 (3151)
D-2,3-butanediol		87	−9.5 (3130)	
meso-2,3-butanediol		69	−9.2 (3131)	
cis-1,2-cyclohexanediol		85	−9.0 (3137)	
trans-1,2-cyclohexanediol		69	−9.4 (3139)	
2,3-dimethyl-2,3-butanediol		39	−10.2 (3122)	
phenyl-1,2-ethanediol		70	−8.6 (3161)[b]	−8.6 (3130)[b]
3-methoxy-1,2-propanediol		58	−8.6 (3173)[b]	−9.1 (3128)[b]
		Triols		
glycerol (1,2-isomer)		79	−7.1 (3109)	−8.7 (3220)
1,2,4-butanetriol (1,2-isomer)		87	−7.6 (3116)	−8.6 (3220)
		Alditols[c]		
erythritol	(1,2-isomer (89%))	66	−6.1 (3200)	−8.3 (3177)
	(2,3-isomer (11%))		−7.7 (3176)	
DL-threitol	(1,2-isomer (40%))	56	−7.2 (3167)	−8.6 (3244)
	(2,3-isomer (60%))		−7.6 (3184)	
ribitol	(1,2-isomer (83%))	68	−5.8 (3220)	−7.9 (3180)
	(2,3-isomer (17%))		−7.4 (3203)[b]	−7.7 (3191)[b]
xylitol	(1,2-isomer (14%))	42	−6.5 (3200)[d]	−8.8 (3200)[d]
	(2,3-isomer (86%))		−7.7 (3198)[b]	−8.1 (3190)[b]
galactitol	(1,2-isomer (11%))	83	−7.0 (3116)	−8.9 (3303)
	(2,3-isomer (71%))		−7.9 (3166)[b]	−8.3 (3238)[b]
	(3,4-isomer (18%))		−8.0 (3221)	
D-mannitol	(1,2-isomer (<1%))	86		
	(2,3-isomer (17%))		−6.2 (3094)	−7.6 (3328)
	(3,4-isomer (82%))		−8.0 (3198)	

[a] Isolated yields; ^{31}P NMR in CD_2Cl_2 solution; J_{PtP} in hertz; $J_{PP} \approx$ 32–34 Hz in all cases. [b] Data from ABX spin-simulation calculation. [c] Equilibrium solution isomer distributions are given in parentheses. [d] Pt–P coupling constant could not be determined accurately due to overlap with major isomer.

strong intra- and intermolecular hydrogen-bonding interactions which influence both the stability constants and the regioselectivities.

Results

Syntheses. Simple vicinal diols readily react with (LL)Pt(CO_3) (LL = dppp and other diphosphines)[22] in dichloromethane solution to give the corresponding 1,2-diolate complexes (eq 1).

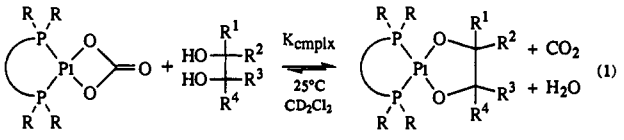

(1)

Like other exchange reactions involving platinum–heteroatom bonds,[23] these reactions are nearly thermoneutral, with typical equilibrium conversions of 10–95% being reached in minutes to hours at room temperature in closed NMR tubes under near-stoichiometric conditions. The reaction is readily reversed by treatment with dry ice, while product formation can usually be driven to completion by utilizing a modest excess of diol and an argon purge. In this manner, a number of new (dppp)Pt(α,β-diolate) complexes have been conveniently isolated in good yield (Table 1, top). This synthetic method is also applicable to the preparation of triolate and alditolate complexes (Table 1, middle and bottom). In the latter case, pyridine is used as the reaction solvent.

(22) dppp = 1,3-bis(diphenylphosphino)propane, dppe = 1,2-bis(diphenylphosphino)ethane, dcpe = 1,2-bis(dicyclohexylphosphino)ethane, dtpe = 1,2-bis(di-*p*-tolylphosphino)ethane, dppv = 1,2-bis(diphenylphosphino)ethene.

(23) Bryndza, H. E.; Fong, L. K.; Paciello, R. A.; Tam, W.; Bercaw, J. E. *J. Am. Chem. Soc.* **1987**, *109*, 1444–1456.

Table 2. Relative K_{cmplx} as a Function of Diol for (dppp)Pt(CO_3)[a]

diol	rel K[b]
2,2-dimethyl-1,3-propanediol	~1
pinacol	100
trans-1,2-cyclohexanediol	100
meso-2,3-butanediol	300
D-2,3-butanediol	700
cis-1,2-cyclohexanediol	700
1,2-propanediol	800
1,2-ethanediol (ED)	≡1000
phenyl-1,2-ethanediol	8000

[a] CD_2Cl_2 solution; total [Pt] = 20–30 mM; total [diol] = 100–300 mM. [b] K((dppp)Pt(ED)) ≡ 1000.

Table 3. Relative K_{cmplx} as a Function of Phosphine[a]

	rel K[b]	
complex[c]	ED[d]	pinacol
$(Ph_3P)_2Pt(CO_3)$	300	
(dcpe)Pt(CO_3)	500	1
(dppp)Pt(CO_3)	≡1000	100
(dtpe)Pt(CO_3)	3000	300
(dppe)Pt(CO_3)	8000	1000
(dppv)Pt(CO_3)	20 000	

[a] CD_2Cl_2 solution; total [Pt] = 20–30 mM; total [diol] = 100–300 mM. [b] K((dppp)Pt(ED)) ≡ 1000. [c] Ligand abbreviations given in ref 22. [d] ED = 1,2-ethanediol.

Complexation Constants. Accurate *absolute* values for the equilibrium diol complexation constants (K_{cmplx}, eq 1) are hard to obtain due to the difficulties of measuring the low solution concentrations of water and carbon dioxide. In contrast, *relative* values for K_{cmplx} are readily determined by allowing mixtures of diols to compete for a single carbonate, and vice versa, and monitoring the reactions by ^{31}P NMR spectroscopy (Tables 2 and 3). For 1,2-ethanediol (ED), equilibrium is achieved at room temperature in less than 1 h, while in the case of the bulky diol pinacol (2,3-dimethyl-2,3-butanediol), 24 h are required. Diolate/diol exchange reactions (e.g., (dppp)Pt(1,2-ethanediolate) + 1,2-propanediol ⇌ (dppp)Pt(1,2-propanediolate) + 1,2-ethanediol) can also be used to determine relative complexation constants. The reproducibility of the relative K values from different experiments was about ±15%.

Regioselectivity. An intermolecular competition reaction showed that the complexation of 1,2-diols is better than that of a typical 1,3-diol by about a factor of 100–1000 (Table 2). For the triols glycerol and 1,2,4-butanetriol, this becomes an intramolecular competition, offering two possible regioselectivities—1,2-coordination to give a 2,5-dioxaplatinacyclopentane isomer or 1,3-coordination to give a 2,6-dioxaplatinacyclohexane isomer. With (dppp)Pt(CO_3), both triols are observed to give nearly exclusively the 1,2-bound dioxametallacyclopentane diolate. For glycerol, assignment of the observed complex as the 1,2-bound isomer is readily apparent from the asymmetry of the ^1H, ^{31}P, and ^{13}C NMR spectra and is confirmed by the gated-decoupled carbon NMR, which shows a doublet and a triplet for the two metallacycle carbons (Table 4; the metallacycle diolate carbons are readily identified by their ~12-ppm downfield shift relative to hydroxyl-substituted diol carbons and by their 3–5 Hz P–C couplings).[24] An overnight ^{31}P spectrum of a 0.125 M solution of the glycerolate complex did, however, show a very small singlet at δ −9.7 (J_{PtP} = 2906 Hz) that might correspond to about 0.5% of the isomeric 1,3-bound glycerolate complex, giving a lower limit of 200 for K_{cmplx}(1,2-glycerolate)/K_{cmplx}(1,3-glycerolate). For 1,2,4-butanetriol, assignment of the

(24) These P–C couplings are readily apparent when the phosphines are nonequivalent. When the phosphines are equivalent, the metallacycle carbon ^{13}C signals generally look like singlets. This is due to the $^3J_{PPtOC}$ and $^4J_{PPtOCC}$ couplings having opposite signs (i.e., +5 and −3 Hz), which then give a near-zero value for $|^3J_{PPtOC} + {}^4J_{PPtOCC}|$ in the ^{13}C portion of the AA'XX' second-order spectrum.

Table 4. ^{13}C NMR Data for (dppp)Pt(diolate) Complexes[a]

	δC_A	δC_B	δC_α[b]	J_{PtC_α}	other diolate C signals
Diols					
1,2-ethanediol (ED)	76.7 (t)[c]				
1,2-propanediol	81.9 (t; 5, 3)	80.7 (d; 5, 3)	20.6 (q; 2)	28	
D-2,3-butanediol	85.1 (d)[c]		23.2 (q)[c]	32	
meso-2,3-butanediol	82.7 (d)[c]		18.3 (q)[c]	24	
cis-1,2-cyclohexanediol	83.6 (d)		33.3 (t)	22	23.6 (t)
trans-1,2-cyclohexanediol	88.8 (d)[c]		36.1 (t)[c]	55	26.3 (t)[c]
2,3-dimethyl-2,3-butanediol	84.8 (s)[c]		28.0 (q)[c]	25	
phenyl-1,2-ethanediol	87.1 (d; 2[d])	83.4 (t; 2[d])	146.5 (s; 2[d])	*e*	127.7, 127.2, 125.9
3-methoxy-1,2-propanediol	83.2 (d; 5, 3)	77.7 (t; 5, 3)	76.8 (t)	14	59.1 (q)
Triols					
glycerol (1,2-isomer)	83.1 (d; 6, 3)	77.7 (t; 6, 3)	65.1 (t)	10	
1,2,4-butanetriol (1,2-isomer)	86.5 (d; 6, 3)	80.5 (t; 5, 3)	34.5 (t; 1)	24	62.7 (t)
Alditols					
erythritol (1,2-isomer (89%))	84.7 (d; 3, 5)	76.8 (t; 6, 3)	73.0 (d)	≈0	62.3 (t)
(2,3-isomer (11%))	84.2 (d)		62.4 (t)	≈20[e]	
threitol (1,2-isomer (40%))	84.4 (d; 5, 3)	77.8 (t; 6, 3)	71.9 (d)	≈9	66.3 (t)
(2,3-isomer (60%))	84.0 (d)		66.9 (t)	≈0	
ribitol (1,2-isomer (83%))	84.3 (d; 4, 3)	76.4 (t; 6, 3)	76.0 (d)	≈0	69.2 (d), 66.5 (t)
(2,3-isomer (17%))	88.2 (d; br)	~84.3[f] (d)[c]	70.8 (d), 65.3 (t)	*e*	62.4 (t)
xylitol (1,2-isomer (14%))	81.3 (d; br)	78.1 (t; br)	72.9 (d)	*e*	71.8 (d), 63.2 (t)
(2,3-isomer (86%))	85.2 (d; 4, 2)	83.9 (d; 4, 2)	73.0 (d), 66.4 (t)	≈8, 10[e]	65.6 (t)
galactitol (1,2-isomer (11%))	83.4[f] (d)[c]	78.4 (t)[c]	76.8 (d)[c]	*e*	73.4[f] (d),[c] 72.3 (d),[c] 65.2 (t)[c]
(2,3-isomer (71%))	86.8 (d; br)	83.4 (d; br)	73.4 (d), 66.1 (t)	*e*, 17	73.3 (d), 64.9 (t)
(3,4-isomer (18%))	85.8 (d)		70.8 (d)	*e*	67.2 (t)
mannitol (1,2-isomer (<1%))	*e*	*e*	*e*	*e*	*e*
(2,3-isomer (17%))	85.2 (d; 4, 4)	82.1 (d; 5, 2)	69.7 (d; 2), 64.1 (t)	≈28, 10[e]	75.4 (d), 62.1 (t)
(3,4-isomer (82%))	85.9 (d)		73.1 (d)	≈0	64.0 (t)

[a] CD_2Cl_2 solution; C_A and C_B, metallacycle carbons; C_α, metallacycle substituent carbon(s); gated-decoupled C–H multiplicities given in parentheses along with J_{PC} in hertz if observable. [b] Assignments of C_α tentative in some cases where J_{PtC} was not observed. [c] Gated-decoupled multiplicity not experimentally determined. [d] $|J_{P_AC} + J_{P_BC}|$. [e] S/N too poor for accurate determination. [f] Signal obscured, deduced from integration.

observed product as the 1,2-isomer was made by a partial analysis of the proton–proton coupling patterns (see Experimental Section), which show that the C3 hydrogens are α to the free hydroxyl group, not β as they would be in the 1,3-isomer. (A 1,4-isomer with a metallacycloheptane ring is ruled out by the gated-decoupled carbon NMR, which again shows a doublet and a triplet for the metallacycle carbons.) For this complex, no extra ^{31}P NMR peaks potentially attributable to either a 1,3- or a 1,4-bound isomer could be identified (detection limit ≈ 1%).

For alditols, the number of significant observed isomers is equal to that expected for complexation via the different vicinal diol units present. The observed isomer ratios, illustrated in Figure 1, reflect thermodynamic equilibria, not kinetic product distributions, equilibration being fast on the laboratory time scale but slow on the NMR time scale (see Discussion). The two C_4 alditols exhibit opposite complexation regioselectivities. The major erythritolate isomer (89%) is unambiguously identified as the 1,2-isomer by its asymmetric ^{31}P NMR spectrum and by a complete assignment of all the alditolate proton–proton coupling constants (see Experimental Section). The minor isomer (11%) is the symmetric 2,3-isomer. For the threitolate complex, the major isomer is easily proven to be the symmetric 2,3-isomer (60%), while the minor isomer is presumed to be the 1,2-isomer (40%) rather than the 1,3-isomer (^1H spectra were too overlapped, even in a 2D COSY, to permit adequate analysis of the proton–proton couplings). The C_5 alditol complexation isomer ratios (ribitol, 83:17; xylitol, 86:14), while superficially identical, again reflect inverse regioselectivities. Thus, gated-decoupled ^{13}C NMR spectra show that the 83% ribitol isomer is the 1,2-isomer and the 86% xylitol isomer is the 2,3-isomer.[25] For the hexitols mannitol and galactitol, one of the three vicinal platinum diolates is present in greater than 70% selectivity in both cases. For mannitol this is the symmetrical 3,4-bound isomer, while for galactitol it is the 2,3-bound isomer. At higher metal-to-alditol ratios, disubstituted complexes can also form, especially in the case of galactitol, for which the poorly soluble 2,3:4,5-bound isomer has been isolated.

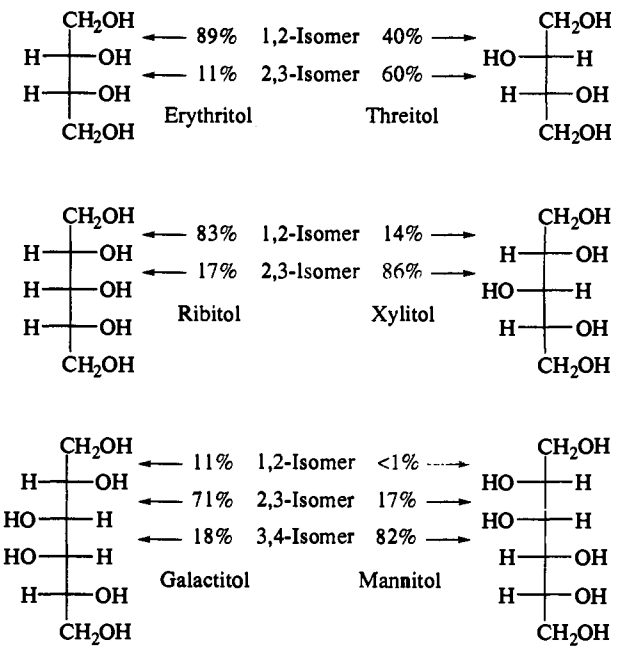

Figure 1. Alditol structures and observed equilibrium complexation regioselectivities for derived (dppp)Pt(alditolate) complexes in CD_2Cl_2.

X-ray Structure of (dppp)Pt(3,4-mannitolate)·(CH_2Cl_2). The solid-state structure of the (dppp)Pt(mannitolate) complex has been determined by single-crystal X-ray diffraction. An ORTEP[26] stereoview is shown in Figure 2, and selected bond distances and angles are given in Tables 5 and 6. The mannitolate dianion is coordinated via the central O3 and O4 oxygen atoms, cor-

(25) All pentitolate and hexitolate complexes are assumed to be vicinal isomers, based on the absence of significant amounts of any other type of isomer in the triolates and tetritolates.

(26) Johnson, C. K. ORTEPII. Report ORNL-5138, Oak Ridge National Laboratory: Oak Ridge, TN, 1976.

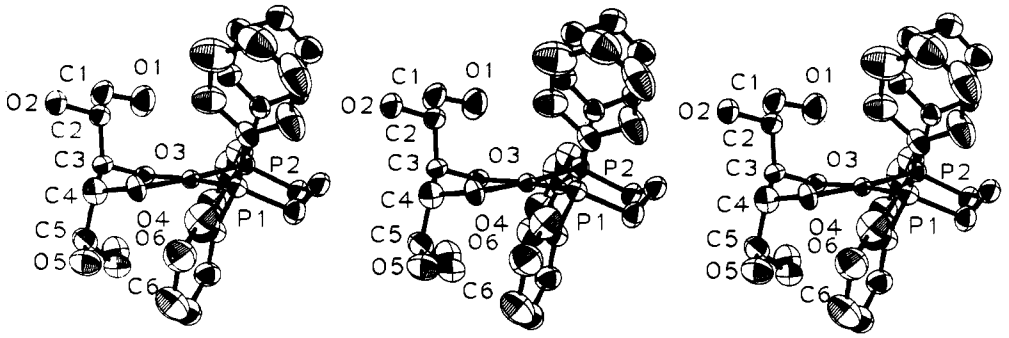

Figure 2. Stereoimages of (dppp)Pt(3,4-D-mannitolate) (left pair cross-eyed, right pair parallel, thermal ellipsoids drawn at 50% probability).

Table 5. Selected Distances (Å) in (dppp)Pt(D-mannitolate)·CH_2Cl_2

Pt–P1	2.216(4)	C4–O4	1.49(2)	C5–C6	1.51(3)
Pt–P2	2.230(4)	C5–O5	1.44(2)	O1···O3	2.66(2)
Pt–O3	2.042(9)	C6–O6	1.42(2)	O3···O6	2.65(2)
Pt–O4	2.033(9)	C1–C2	1.60(3)	O4···O5	2.65(2)
C1–O1	1.42(2)	C2–C3	1.53(2)	O2···O5′	3.07(2)
C2–O2	1.45(2)	C3–C4	1.54(2)	O1···Cl1	3.37(2)
C3–O3	1.42(2)	C4–C5	1.53(2)	O2···Cl2	3.58(2)

Table 6. Selected Angles (deg) in (dppp)Pt(D-mannitolate)·CH_2Cl_2

P1–Pt–P2	93.7(1)	O3–C3–C4	109(1)	O2–C2–C3	110(1)
P1–Pt–O4	88.6(3)	C3–C4–O4	109(1)	O3–C3–C2	110(1)
P2–Pt–O3	93.9(3)	C1–C2–C3	107(1)	O3–C3–C4	109(1)
O3–Pt–O4	83.9(4)	C2–C3–C4	111(1)	O4–C4–C3	109(1)
P1–Pt–O3	172.3(3)	C3–C4–C5	115(1)	O4–C4–C5	109(1)
P2–Pt–O4	175.3(3)	C4–C5–C6	118(1)	O5–C5–C4	105(1)
Pt–O3–C3	109.2(8)	O1–C1–C2	110(1)	O5–C5–C6	105(1)
C4–O4–Pt	109.7(8)	O2–C2–C1	105(1)	O6–C6–C5	111(1)

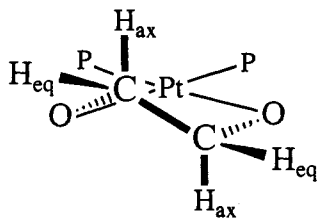

Figure 3. Illustration of the 2,5-dioxaplatinacyclopentane ring and substituent geometries.

responding to the major isomer present in solution. The resulting 2,5-dioxaplatinacyclopentane chelate ring exhibits a twist conformation with two axially disposed dihydroxyethyl substituents (cf. Figures 2 and 3). The angle between the O3–Pt–O4 and C3–Pt–C4 planes is 24°, with C3 displaced 0.48 Å above the O3–Pt–O4 plane and C4 displaced 0.13 Å below the plane. The twist conformation and axial substitution pattern are similar to those determined structurally for (1,2-C_6H_4(PPhMe)$_2$)Pt(1,2-glycerolate), the sole previously reported organo-transtion-metal complex of an unprotected carbohydrate.[13] In fact, there appear to be less than a dozen crystallographically characterized complexes of any transition metal with a native, oxygen-bound carbohydrate.[27] The dppp chelate ring on the opposite side of the square-planar platinum exhibits a slightly flattened chair cyclohexane conformation, analogous to that found for 20 of the 24 dppp chelate structures contained in the Cambridge Structural Database.[28] The axial ("top" or "inner") phenyl groups are arranged in a quasiparallel π–π stacking fashion, with an interphenyl separation of about 4–6 Å, while the equatorial ("bottom" or "outer") phenyl groups are nearly coplanar with each other and perpendicular to the axial phenyls.

Four different hydrogen-bonding interactions are present in the complex, three intramolecular and one intermolecular. The terminal O1 hydroxyl group of the C1–C2 dihydroxyethyl group is intramolecularly hydrogen-bonded via a 6-membered ring to the Pt-bound O3 oxygen from above the Pt coordination plane (O1···O3 = 2.66(2) Å). The secondary O2 hydroxyl group probably participates in a weak intermolecular hydrogen bond to O5 in an adjacent molecule (O2···O5′ = 3.07(2) Å). In contrast, the C5–C6 dihydroxyethyl group has both hydroxyls strongly hydrogen-bonded to the Pt-bound oxygens from below the Pt coordination plane, creating fused 5- and 7-membered hydrogen-bonded ring systems involving O5 and O6, respectively (O5···O4 = 2.65(2) Å, O6···O3 = 2.65(2) Å).

The only other reported structures for mannitol complexes of transition metals are the sodium salt of [Mo_2O_5(O_3(OH)-C_6H_8(OH)$_2$)]$^-$ [29] and the ammonium salt of the same anion.[30] In both cases, the mannitol is present as the 2,3,4-trianion, with the hydroxyl oxygen on C1 and the alkoxide oxygen on C3 bridging the two molybdenums. The alkoxide oxygens on C2 and C4 are terminally bonded to different molybdenums, while the oxygens on C5 and C6 are uncoordinated. Extensive intermolecular hydrogen-bonding involving both the mannitolate ligand and water solvent molecules is present in both structures, as well as the ammonium ion in the latter.

Discussion

Syntheses. In the past, metal diolate complexes have usually been prepared from corresponding bis(alkoxide) complexes by alcohol exchange (eq 2).[13,17,21] The intermediate alkoxide com-

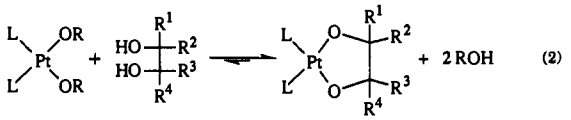

(2)

plexes are invariably quite water-sensitive and are also often unstable with respect to β-hydrogen elimination,[31] limiting their utility as precursors. Reports that complexes derived from weak carbon acids, such as β-ketoesters,[32] can be prepared by reaction with bis(phosphine)platinum carbonates suggested that diols might behave similarly. This led us to develop the convenient new synthetic method illustrated in eq 1. The carbonate precursors can be prepared by a number of methods[33–36] and are easy to store and handle due to their air and water stability. The reaction

(27) A search of the Cambridge Structural Database (April, 1993 release) for the fragment TR-O-C($H_{1/2}$)-C($H_{1/2}$)-O gave only the following hits (identified by their codes) that involved native carbohydrates: GETKUL, LYXSMO, MANMOL10, MNGLUD, QQQAZD01, SIRDIG, SIRDOM, VOWKOH, XMANMO.

(28) Allen, F. H.; Davies, J. E.; Galloy, J. J.; Johnson, O.; Kennard, O.; Macrae, C. F.; Mitchell, E. M.; Mitchell, G. F.; Smith, J. M.; Watson, D. G. *J. Chem. Inf. Comput. Sci.* **1991**, *31*, 187.

(29) Hedman, B. *Acta Crystallogr.* **1977**, *B33*, 3077–3083.

(30) Godfrey, J. E.; Waters, J. M. *Cryst. Struct. Commun.* **1975**, *4*, 5–8.

(31) Bryndza, H. E.; Tam, W. *Chem. Rev.* **1988**, *88*, 1163–1188.

(32) Clarke, D. A.; Kemmitt, R. D. W.; Mazid, M. A.; McKenna, P.; Russell, D. R.; Schilling, M. D.; Sherry, L. J. S. *J. Chem. Soc., Dalton Trans.* **1984**, 1993–2002 and references therein.

(33) Hayward, P. J.; Blake, D. M.; Wilkinson, G.; Nyman, C. J. *J. Am. Chem. Soc.* **1970**, *92*, 5873–5878.

(34) Miyamoto, T. K.; Suzuki, Y.; Ichida, H. *Bull. Chem. Soc. Jpn.* **1992**, *65*, 3386–3397.

byproducts, water and carbon dioxide, are easily removed upon workup, as is any excess starting diol in most cases. Only when the complexation constant is very low, e.g., for (dcpe)Pt(pinacolate) and (dppp)Pt(2,2-dimethyl-1,3-propanediolate), is it necessary to resort to the tedious and less general but more thermodynamically favorable alcohol-exchange route.

Solution Conformations. The multiple NMR spins (^{1}H, ^{31}P, ^{13}C, ^{195}Pt) present in these L_2Pt(diolate) complexes provide a powerful tool for analyzing their solution conformations and hydrogen-bonding interactions. While a detailed analysis of these findings will be presented elsewhere,[37] one useful structural correlation is worth noting here. A Karplus-type dihedral angle dependence[38] has been observed for the three-bond ^{195}Pt–X–C–^{1}H coupling in platinum(II) amine (X = N)[39,40] and sulfide (X = S)[41,42] complexes. A similar situation appears to hold for ^{195}Pt–O–C–$^{13}C_\alpha$ couplings (cf. Table 4),[43] which are more readily determined in the present situation than ^{195}Pt–O–C–^{1}H couplings. The latter are broadened not only by ^{195}Pt chemical shift anisotropy[44] but also by H–H coupling and are also often obscured by overlapping signals.

The C_α carbons in (dppp)Pt(*trans*-1,2-cyclohexanediolate), which are locked in an equatorial position by the bicyclic ring system, have $^3J_{PtOCC_\alpha}$ = 55 Hz for a PtOCC$_\alpha$ angle of ca. 165°. The corresponding *cis*-1,2-cyclohexanediolate isomer, the (dppp)Pt(*meso*-2,3-butanediolate), and the (dppp)Pt(pinacolate), which all have α-carbons with equal time-averaged occupancies in both axial and equatorial positions, have $^3J_{PtOCC_\alpha} \approx 25$ Hz. From this we deduce that axial C_α carbons, with a PtOCC$_\alpha$ angle of ca. 85°, must have $^3J_{PtOCC_\alpha} \approx -5$ Hz ((55 + (−5))/2 = 25). Based on these $^3J_{PtOCC_\alpha}$ values, the solution conformational composition of related alkyl-substituted complexes can be estimated. For example, the (dppp)Pt(1,2-propanediolate) complex is calculated to be a ca. 55:45 mixture of rapidly equilibrating equatorial and axial conformers, respectively (ΔG = 0.12 kcal/mol). Similarly, the D-2,3-butanediolate is estimated to be a ca. 62:38 mixture of diequatorial and diaxial conformers (ΔG = 0.29 kcal/mol). From this it can be concluded that the axial–equatorial energy difference in the (dppp)Pt(diolate) series is about 0.15 kcal/mol per methyl substituent, favoring equatorial substitution.

A comparable quantitative analysis of the conformations of complexes with α-oxygen substituents will require data from suitable model compounds of known geometry because the Karplus relationship can be affected by the electronegativity of neighboring substituents.[45,46] The near-zero value for $^3J_{PtC_\alpha}$ in the 3,4-mannitolate complex is consistent, however, with a nearly complete preference for axial substitution, the conformation observed in the solid-state X-ray structure. Values for $^3J_{PtC_\alpha}$ for the 2,3-erythritolate and 2,3-mannitolate complexes (Table 4), which are currently poorly determined due to signal-to-noise problems with these minor isomers, suggest that $^3J_{PtC_\alpha}$(equatorial) + $^3J_{PtC_\alpha}$(axial) ≈ 40 Hz, hence $^3J_{PtC_\alpha}$(equatorial) ≈ 40–50 Hz. If so, the glycerolate complex ($^3J_{PtC_\alpha}$ = 10 Hz) is about 70% axially substituted in solution. Axial substitution in the glycerolate vs the equatorial preference observed in the 1,2-propanediolate may occur in order to permit formation of a favorable 6-membered hydrogen-bonding ring to the β-Pt-bound oxygen. A weaker 5-membered hydrogen-bonding ring to the α-Pt-bound oxygen would result from an equatorial glycerolate conformation (*vide infra*). The preference for axial substitution in complexes with α-oxygen substituents does not appear to be solely due to hydrogen-bonding effects, however, since the 3-methoxy-1,2-propanediolate complex, a non-hydrogen-bonding model for the glycerolate, also has a low value for $^3J_{PtC_\alpha}$ (14 Hz). The 1,2,4-butanetriolate complex, which has a β-oxygen substituent, is more nearly an equal mixture of axial and equatorial conformers ($^3J_{PtC_\alpha}$ = 24 Hz). All of these conformational results are consistent with conclusions derived from $^3J_{PtOCH}$ values for cases where these have been determined.[37]

Hydrogen Bonding. The *intra*molecular solid-state O···O hydrogen bond distances of 2.65(2) Å found here in the (dppp)Pt(mannitolate) complex are among the shortest observed for nonionic O–H···O hydrogen bonds.[47] Analogous *inter*molecular hydrogen-bonding interactions have been observed in other late-transition-metal alkoxide complexes,[13,48–50] but those have primarily involved more acidic hydrogen-bonding acids such as phenols and fluoroalcohols. Particularly relevant are $Rh(PMe_3)_3$(O-*p*-tolyl)·(HO-*p*-tolyl) (O···O = 2.62 Å)[48] and $C_6H_4(PPhMe)_2$)Pt(glycerolate)·2MeOH (O···O = 2.65–2.67 Å).[13] In the former complex, the enthalpy of formation for the hydrogen-bonded adduct has been determined to be 14 kcal/mol. In the latter complex, the hydrogen-bonding involves both glycerolate–glycerolate and glycerolate–methanol interactions. These strong hydrogen bonds are a natural consequence of the marked $M^{\delta+}$–$O^{\delta-}$ polarization present in late-metal alkoxides.[31,51]

While accurate characterization of the hydrogen bond geometries in these compounds will require investigation by single-crystal neutron diffraction techniques, it is already apparent that there are significant variations in the details of these diolate hydrogen bonds. For example, (dppp)Pt(3,4-mannitolate) exhibits three different-sized intramolecular hydrogen-bonded rings (5–7 membered), with two hydrogen bonds to one diolate oxygen and only one hydrogen bond to the other diolate oxygen. Double intramolecular hydrogen-bonding by the axial mannitolate C1–C2 dihydroxyethyl group, analogous to that observed for the C5–C6 dihydroxyethyl group, would appear to be precluded by unfavorable interactions that would result between the C1–C2 fragment and the axial ("top") dppp–chelate phenyl groups. In contrast, the equatorial ("bottom") phenyls have a parallel orientation which places them out of the way of the doubly hydrogen-bonded C5–C6 dihydroxyethyl group. In solution, the two types of dihydroxyethyl groups are time-average equivalent. This equilibration probably occurs via inversion of the dppp "cyclohexane" chelate ring and concurrent phenyl group rotation and axial–equatorial interchange, together with an exchange in the hydrogen-bonding modes of the two dihydroxyethyl groups. Single-crystal X-ray structures of the (dppp)Pt(1,2-glycerolate), (dppp)Pt(1,2-erythritolate), and (dppp)Pt(2,3-galactitolate) complexes show that these compounds also exhibit axial metallacycle substitution with varying hydrogen-bonding features.[52]

NMR spectra demonstrate that the strong hydrogen bonds observed in the solid-state alditolate structures are a pervasive

(35) Anderson, G. K.; Lumetta, G. J.; Siria, J. W. *J. Organomet. Chem.* **1992**, *434*, 253–259.

(36) The carbonates employed here were prepared from the corresponding dichloride by reaction with silver carbonate in *wet* dichloromethane or by sequential treatment with sodium isopropoxide, water, and carbon dioxide (see Experimental Section). A more complete study of platinum carbonate complexes will be reported elsewhere (Andrews, M. A.; Koenig, K. S.; Gould, G. L.; Voss, E. J., work in progress).

(37) Andrews, M. A.; Voss, E. J., work in progress.

(38) Karplus, M. *J. Am. Chem. Soc.* **1963**, *85*, 2870–2871.

(39) Erickson, L. E.; McDonald, J. W.; Howie, J. K.; Clow, R. P. *J. Am. Chem. Soc.* **1968**, *90*, 6371–6382.

(40) Appleton, T. G.; Hall, J. R. *Inorg. Chem.* **1971**, *10*, 1717–1725.

(41) Haake, P.; Turley, P. C. *J. Am. Chem. Soc.* **1967**, *89*, 4611–4616.

(42) Turley, P. C.; Haake, P. *J. Am. Chem. Soc.* **1967**, *89*, 4617–4621.

(43) None of the metallacycle carbons exhibits a measurable coupling to platinum, hence $^2J_{PtOC} \approx -^3J_{PtOCC}$.

(44) The ^{195}Pt satellites are significantly broadened because of rapid relaxation due to large chemical shift anisotropies (see: Ismail, I. M.; Kerrison, S. J. S.; Sadler, P. J. *Polyhedron* **1982**, *1*, 57–59).

(45) Haasnoot, C. A. G.; de Leeuw, F. A. A. M.; Altona, C. *Tetrahedron* **1980**, *36*, 2783–2792.

(46) Kalinowski, H.-O.; Berger, S.; Braun, S. *Carbon-13 NMR Spectroscopy*; Wiley: NY, 1988.

(47) Steiner, T.; Saenger, W. *Acta Crystallogr.* **1992**, *B48*, 819–827.

(48) Kegley, S. E.; Schaverien, C. J.; Freudenberger, J. H.; Bergman, R. G.; Nolan, S. P.; Hoff, C. D. *J. Am. Chem. Soc.* **1987**, *109*, 6563–6565.

(49) Osakada, K.; Ohshiro, K.; Yamamoto, A. *Organometallics* **1991**, *10*, 404–410.

(50) Lunder, D. M.; Lobkovsky, E. B.; Streib, W. E.; Caulton, K. G. *J. Am. Chem. Soc.* **1991**, *113*, 1837–1838.

(51) Mayer, J. M. *Comments Inorg. Chem.* **1988**, *8*, 125–135.

(52) Klooster, W. T.; Voss, E. J.; Koetzle, T. F.; Andrews, M. A., work in progress to be reported elsewhere.

feature of these complexes in solution as well.[13] The ^{1}H NMR resonances of the hydroxyl protons in the (dppp)Pt glycerolate and 1,2,4-butanetriolate complexes in CD_2Cl_2 are found at 2.48 and 5.15 ppm, respectively, well downfield of that observed for non-hydrogen-bonded alcohol protons (e.g., 1.28 ppm for 5 mM Me_2CHOH in the same solvent). These hydroxyl proton chemical shifts are essentially independent of concentration (<0.05 ppm shift from 1 to 125 mM), indicative of intramolecular hydrogen-bonding. The two nonequivalent $^3J_{HCOH}$ couplings in the diastereotopic C^*CH_2OH groups in these and related complexes are also very different, typically 8–10 and 1–3 Hz, evidence for strong rotational preferences induced by the intramolecular hydrogen bonds.

The chemical shifts of the (dppp)Pt(3,4-mannitolate) complex's hydroxyl protons are remarkably comparable to those found in the model triolate complexes; the solution-equivalent secondary O2 and O4 α-hydroxyl protons appear as a doublet at δ 2.02, while the terminal O1 and O6 β-hydroxyl protons appear as a doublet of doublets at δ 5.11. The δ 5.11 signal is independent of concentration, consistent with strong intramolecular hydrogen-bonding, while the δ 2.02 signal shifts downfield to δ 2.47 upon increasing the concentration from 1 to 70 mM, as expected for at least some contribution from intermolecular hydrogen-bonding. All of these observations are in accord with the solid-state structure. The ^{1}H NMR spectrum of the corresponding (dcpe)-Pt(mannitolate) complex[22] is completely analogous in all respects, proving that the unusual characteristics of the hydroxyl–proton resonances in these complexes are in fact due to hydrogen-bonding, not ring current proximity effects of the phosphine phenyl groups. The proton NMR of the (dppp)Pt(1,2-erythritolate) complex is also comparable, having hydroxyl resonances at 1.88 (secondary α-hydroxyl) and 6.19 ppm (primary β-hydroxyl), both absorbances now being concentration independent. These resonances do show a distinct temperature dependence, the former shifting slightly upfield to 1.75 ppm and the latter markedly downfield to 6.60 at ca. 250 K. Since downfield shifts on cooling are the norm for hydrogen-bonded hydroxyl protons,[53] the upfield shift of the secondary α-hydroxyl may reflect a weakening of this hydrogen bond at low temperatures to permit a more favorable conformation for the apparently stronger hydrogen bond formed by the primary β-hydroxyl. This greater strength for hydrogen bonds involving primary β-hydroxyls (7-membered ring) over that of secondary α-hydroxyls (5-membered ring) in the mannitolate and erythritolate complexes is consistent with the shifts observed in infrared O–H stretching frequencies for intramolecular hydrogen-bonded α,ω-diols: 32 cm^{-1} for 1,2-ethanediol (5-membered ring), 78 cm^{-1} for 1,3-propanediol (6-membered ring), and 156 cm^{-1} for 1,4-butanediol (7-membered ring).[54]

Hydrogen-bonding also appears to affect the ^{31}P chemical shifts and ^{195}Pt–^{31}P coupling constants. The data in Table 1 yield a roughly linear correlation between δP_A and J_{PtPB}, and vice versa, both generally tending toward more positive values in the intramolecularly hydrogen-bonded triolate and alditolate complexes ($J_{PtPB} = 53\delta P_A + 3600$, $R = 0.8$ (see Figure S-1 in the supplementary material)). This effect could simply be attributed to the lower basicity of alditolate anions compared to the diolate anions and hence a decreased Pt–P bond length and a greater value for the trans Pt–P coupling constant.[55] Hydrogen-bonding to the diolate oxygen should further lower its basicity, however. Thus, sequential addition of aliquots of diols or alcohols to the simple diolate complexes results in changes in both δP and Pt–P coupling constants, which we attribute to intermolecular hydrogen bond formation. For example, Figure 4 shows a plot of one of

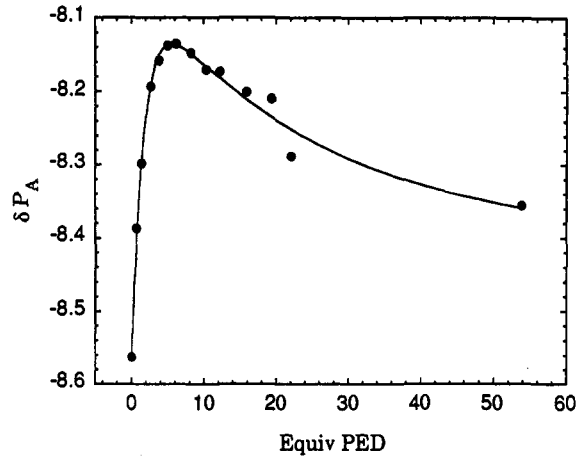

Figure 4. ^{31}P NMR chemical shift of P_A of (dppp)Pt(1,2-phenylethanediol) (26.9 mM in CD_2Cl_2) as a function of added 1,2-phenylethanediol. The curve, drawn as an aid to the eye, is a double-exponential fit to the data.

the ^{31}P NMR chemical shifts of (dppp)Pt(phenyl-1,2-ethanediolate) as a function of added phenyl-1,2-ethanediol in CD_2Cl_2. The presence of an inflection point suggests that at least two sequential interactions with different binding constants must be present, a not unexpected result based on the multiple hydrogen bonds observed in the mannitolate X-ray structure. Quantitative analysis of these ^{31}P trends will require more detailed investigation but could provide significant information regarding the strengths of these hydrogen bonds.

Hydrogen-bonding considerations seem to be a factor even in the syntheses of these complexes. Better results are obtained in non-hydrogen-bonding solvents, particularly dichloromethane, than in polar solvents such as pyridine, for which equilibrium conversions appear to be lower under comparable conditions. Carbon dioxide has a similar solubility in halogenated solvents and pyridine,[56] and the small amount of water formed in these reactions does not exceed the solubility limit, determined to be about 0.1 M in CD_2Cl_2. Since this rules out the obvious participants in the equilibrium, we attribute the poorer results in pyridine to the disruption of key hydrogen-bonding interactions between the diol and the product diolate. Consistent with this hypothesis is the observation that small excesses of diol greatly facilitate the reaction over those carried out at the nominal 1:1 stoichiometry. The syntheses of alditolate complexes, which cannot be prepared in dichloromethane because of alditol solubility constraints, nevertheless proceed well in pyridine. Here the higher alditol OH acidities and the strong intramolecular hydrogen bonds present in the product alditolates apparently allow for high complexation constants.

Complexation Constants. An elegant study by Bryndza, Bercaw, and co-workers[23] shows that exchange reactions of the type $L_nMX + HY \rightleftharpoons L_nMY + HX$ are often nearly thermoneutral (including L_nM = (dppe)PtMe), hence the differences in M–X and M–Y bond dissociation energies (BDEs) must be the same as the differences in H–X and H–Y BDEs. If this same relationship were rigorously true in the present case, our relative diol complexation constants, K_{rel} (eq 1), would necessarily all be equal. Instead, the experimental relative diol complexation constants (Tables 2 and 3) span a total range of over 10^4 [(dcpe)-Pt(pinacolate) = 1 to (dppv)Pt(ethanediol) = 20 000], with a projected range of over 10^5 [(dcpe)Pt(pinacolate) = 1 to (dppv)-Pt(phenylethanediol) $\approx$ 160 000, the latter estimated by taking 20 000 for (dppv)Pt(ethanediol) and multiplying by a factor of 8 based on the relative K_{cmplx} for (dppp)Pt(phenylethanediol) vs (dppp)Pt(ethanediol)]. Deviations in K_{rel} of a similar size were

(53) Tucker, E. E.; Lippert, E. In *The Hydrogen Bond. Recent Developments in Theory and Experiments. II. Structure and Spectroscopy*; Schuster, P., Zundel, G., Sandorfy, C., Eds.; North-Holland Publishing Company: New York, 1976; Vol. 2, pp 793–830.
(54) Kuhn, L. P. *J. Am. Chem. Soc.* **1952**, *74*, 2492–2499.
(55) Pregosin, P. S. *Coord. Chem. Rev.* **1982**, *44*, 247–291.
(56) Fogg, P. G. T.; Gerrard, W. *Solubility of Gases in Liquids*; Wiley: New York, 1991; pp 246–264.

noted in the Bryndza and Bercaw work, but for much less closely related HX/HY pairs. The deviations were ascribed to multiple M–Y bonding (e.g., $K > 1$ for Y = CN) or M ↔ Y steric interactions (e.g., $K < 1$ for Y = NPh_2) not present in H–X. The authors' closing comments noted that these small thermodynamic deviations could nevertheless produce marked changes in product selectivities, as is clearly demonstrated here.

Multiple factors influence K_{cmplx}. For a series of diolate complexes with the same phosphine, these include the stabilities of both the starting diol and the product diolates, which are in turn a function of steric, electronic, and hydrogen-bonding interactions. For a series of complexes with different phosphines, steric factors in the diolate complexes and electronic factors in both the carbonates and diolates come into play. In the case of both diols and phosphines, these factors can be manifested as a chelate ring-size effect. These chelate ring-size effects are particularly apparent from the data. Thus, 1,2-diol chelation is favored over 1,3-diol chelation by 2–3 orders of magnitude. This result is consistent with both the greater stability of 6-membered vs 5-membered hydrogen-bonded rings in the starting 1,3-diol vs 1,2-diol[54] and with the converse greater stability of 5-membered metallacycle chelates over 6-membered chelates in the product diolates.[57] Interestingly, an indirect *phosphine* chelate ring-size effect on K_{cmplx} is also observed, with diol complexation being favored by auxiliary 1,2-diphosphines (dppe) over corresponding 1,3-diphosphines (dppp) by about 1 order of magnitude.

Electronic effects are evident from the observation that electron-donating substituents on both the diol and the phosphine inhibit diol complexation. Thus there is about a 0.2–0.4 kcal/mol decrease in ΔG for complexation per added diol methyl group in the (dppp)Pt series. The higher binding constant for phenyl-1,2-ethanediol over 1,2-ethanediol is also consistent with this trend. In the case of the phosphine auxiliary ligand, the inhibition of diol binding by electron-donating substituents is supported by an inverse correlation between the enthalpies of diprotonation of the phosphine ligand and K_{rel}. Thus ($\Delta H_{HP1} + \Delta H_{HP2}$) is –29.9 kcal/mol for dppv, –43.0 kcal/mol for dppe, and –45.8 kcal/mol for dppp,[58] corresponding to our K_{rel} values of 20:8:1, respectively. Similarly, a factor of 3 decrease in K_{cmplx} is observed in going from dppe to its para methyl-substituted analogue dtpe. A large portion of the 16-fold drop in K_{cmplx} observed for the alkyl diphosphine dcpe vs its aromatic analogue dppe is also probably electronic in origin for the sterically undemanding 1,2-ethanediol. With bulkier diols, however, steric effects are readily apparent, with a 2 orders of magnitude difference between the relative binding constants of pinacol to (dppp)Pt and (dcpe)Pt compared to only a factor of 2 difference for 1,2-ethanediol.

An example of the difficulties involved in predicting the relative contributions of different factors to the K_{cmplx} values is provided by a comparison of two pairs of isomeric diols. The D- (or *threo*-) 2,3-butanediol isomer is known to have a stronger intramolecular hydrogen bond than the *meso*- (or *erythro*-) isomer.[54] The product diolate derived from *threo*-2,3-butanediol should also be more stable, however, since it can form a more favorable di-equatorially substituted metallacycle (cf. conformational analyses above) than the *erythro* diol, which necessarily yields an ax,eq metallacycle. The experimentally observed preference resulting from this competition of effects is complexation of the *threo* (D) diol over *erythro* (*meso*) diol by about a factor of 2. In the corresponding cyclic diols, *cis*- and *trans*-cyclohexanediol, the interpretation is even more problematic. The cis diol is known to have a slightly stronger intramolecular hydrogen bond than the trans isomer,[59] and in fused 6/5 hydrocarbon ring systems, the trans isomer is more stable.[60] Despite these two factors, both of which would seem to favor complexation of the trans diol over the cis diol, the surprising experimental result is the reverse, by a factor of 7. Another possible factor is the effects of intermolecular hydrogen-bonding interactions, both diol–diol and diol–diolate, on K_{cmplx} (cf. Figure 4). While a couple of test experiments did show that the relative binding constants were independent of the amount of diol present within experimental error (ca. ±15%), much more thorough quantitative studies will be needed to unravel the contribution of diol–diolate hydrogen-bonding to the observed complexation constants.

Preliminary attempts have also been made to use molecular modeling calculations[61] to help understand these various results. As might be expected, molecular mechanics appeared to reproduce axial–equatorial energy differences of simple diolate complexes fairly well (e.g., a calculated 0.9 kcal/mol ax–eq energy difference for (dppp)Pt(1,2-propanediolate) vs 0.12 kcal/mol observed). The potential errors in the calculation methods are larger, however, when hydrogen-bonding interactions (e.g., intradiol and diol–diolate) are involved, and this was reflected in a failure of the calculations to properly reproduce the observed variations in K_{cmplx}, e.g., for *cis*- vs *trans*-cyclohexanediol.

Regioselectivities. The complexation of polyols provides an intramolecular selectivity competition, which is in principle more amenable to analysis than an intermolecular competition, since the stabilities of the starting materials are no longer a factor. Experimentally, however, a concern arose over whether the alditol complexation regioselectivities determined by ^{31}P NMR (Table 1 and Figure 1) reflected kinetic or thermodynamic product ratios. For the intermolecular competitions, the approach to equilibrium is readily observed over a period of minutes to hours, allowing a clear distinction between kinetic and thermodynamic properties. In the case of the alditols, however, the product ratios were normally independent of time, both during their formation from the carbonate and after dissolution of the pure isolated complex. Variable-temperature NMR experiments with (dppp)Pt(erythritolate) (223–295 K in dichloromethane-d_2 and 295–388 K in pyridine-d_5) showed that the ratio of the 2,3- to the 1,2-isomer varied with temperature. At the lower temperatures, isomer equilibration could now be observed to occur over a period of minutes to hours, while at high temperatures the equilibration was rapid but not yet fast enough to lead to signal-averaging on the NMR time scale. The observed K_{eq} values (2,3- ⇌ 1,2-) ranged from 3.6 to 19. The derived van't Hoff plots give an enthalpy difference between the two isomers of about 2 kcal/mol in both solvents (cf. Figure S-2 in the supplementary material). From this we conclude that the observed isomer ratios at ambient temperature are in fact thermodynamic equilibrium values.

Additional evidence supports equilibration being fast on the laboratory time scale for all of the alditol complexes. First, dissolution of crystals of (dppp)Pt(mannitolate) in dichloromethane and pyridine yields distinctly different regioselectivities, which then do not change over time in either solvent. This proves that rapid isomerization had to have occurred in at least one of the two solvents, and probably both since the solid-state structure appears to be exclusively the 3,4-isomer. Second, the carbonate–diolate equilibria are all readily reversible, including those involving alditols, as are diolate–diol exchange reactions. Indeed, in the closely related complex, $(C_6H_4(P^*MePh)_2)Pt$(glycerolate), diastereomeric equilibration is reported to occur by the time an NMR spectrum could be recorded at –90 °C.[13] In one case in the present system, reaction of (dppe)Pt(CO_3) with mannitol in *N*-methyl-2-pyrrolidinone, there does appear to be a slight observable kinetic preference for formation of the 1,2-isomer at

(57) Martell, A. E.; Calvin, M. *Chemistry of the Metal Chelate Compounds*; Prentice-Hall: Englewood Cliffs, NJ, 1952; pp 134–137, 143.
(58) Sowa, J. R.; Angelici, R. J. *Inorg. Chem.* **1991**, *30*, 3534–3537.
(59) Kuhn, L. P. *J. Am. Chem. Soc.* **1954**, *76*, 4323–4326.
(60) Chang, S.-J.; McNally, D.; Shary-Tehrany, S.; Hickey, M. J.; Boyd, R. H. *J. Am. Chem. Soc.* **1970**, *92*, 3109–3118.
(61) Calculations were carried out with the Personal CAChe software from CAChe Scientific using the built-in augmented MM2 molecular mechanics force field and MOPAC quantum mechanics parameters.

very early reaction times which quickly gives way to a different distribution more strongly favoring the major thermodynamic 3,4-isomer.

The resulting observed equilibrium alditol complexation regioselectivities for the isolated complexes in dichloromethane-d_2, given in Figure 4, represent significant enhancements over statistical expectations (67:33 1,2-:2,3- for tetritols, 50:50 for pentitols, and 40:40:20 1,2-:2,3-:3,4- for hexitols). Complexation is favored at *threo* over *erythro* diol units and in positions that lead to dihydroxyethyl- over hydroxymethyl metallacycle substituents. Thus in mannitol and galactitol, where both *threo* and *erythro* internal diols are present, complexation favors the *threo* position and most strongly so for mannitol, which yields two dihydroxyethyl substituents. Similarly, a higher *threo* selectivity is observed for xylitol than for threitol. When an internal *threo* linkage is not available (erythritol and ribitol), complexation occurs preferentially at the terminal nonstereogenic diol. A direct competition between threitol and erythritol with (dppp)Pt(CO_3) in pyridine also showed a 2-fold preference for complexation of the *threo* isomer, just as in the case of the 2,3-butanediols in dichloromethane. The higher K_{cmplx} for threitol over erythritol reflects a preference for diaxial metallacycle substitution in the *threo* isomer over ax,eq substitution in the *erythro* isomer. This contrasts with the observed preference for diequatorial over ax,eq substitution in the *threo*- vs *erythro*-2,3-butanediols, respectively. In the case of alditols, axial substitution and the presence of dihydroxyethyl substituents may facilitate the formation of especially strong double hydrogen-bonding systems, like that observed crystallographically in the mannitolate complex. As discussed above, hydrogen-bonding via a β-hydroxyl group (7-membered ring) is stronger than that by an α-hydroxyl group (5- or 6-membered ring), again favoring regioselectivities with dihydroxyethyl substitution over hydroxymethyl substitution.

There are no good direct analogues to compare with the presently observed regioselectivities. Complexes of carbohydrates with simple transition-metal ions almost invariably involve polydentate coordination of the carbohydrate substrate, typically tridentate via hydroxyls with a *threo,threo* relationship.[11] Dialkyltin derivatives of carbohydrates are gaining importance in carbohydrate synthetic chemistry[62] and involve a 2,5-dioxastannacyclopentane ring very similar to the platinum compounds reported here. Selective functionalization of different hydroxyls has been achieved by this method[63] but does not yet appear to have been the subject of a systematic investigation. The dialkyltin situation is further complicated by the presence of oligomers.[64] Periodate cleavage of diols is also proposed to proceed via a 5-membered cyclic intermediate, and the selectivities observed for that correspond fairly well with those seen here, namely preferential cleavage at internal *threo* diol units.[65,66] The regioselectivity observed in acetal derivatives of alditols is more complicated and depends on whether the acetal is formed with an aldehyde or a ketone, the former favoring 6-membered rings, the latter 5-membered rings.[67]

Conclusion. Development of a thorough systematic understanding of the marked complexation selectivities observed in the present work is complicated by the small energy differences involved and the large number of possible contributing factors. The latter include not only the usual electronic and steric properties of the metal and its auxiliary ligands but also the chirality at both the metallacycle and the α-exocyclic carbon atoms, the availability of 5-, 6-, and 7-membered hydrogen-bonded ring systems, and solvent polarity and hydrogen-bonding characteristics. Complexation to cyclic sugars will be even more intricate, as evidenced by the changing isomer ratios observed over time on treatment of (dppe)Pt(CO_3) with glucose.[68] In these cyclic sugars, there are additional geometric constraints and the possibility of both pyranose and furanose isomers, each in the α and β configurations.

These same difficulties, however, represent a great opportunity for the development of highly selective organo-transition-metal catalysts and reagents for effecting carbohydrate transformations. Only small energetic changes in the metal–substrate–solvent interactions beyond those already observed are needed to achieve >99% selectivity, and there are many factors available to "tune". For example, switching from dichloromethane to pyridine as solvent increases the selectivity for the 2,3-isomer of (dppp)Pt(galactitolate) from 72% to 84% and for the 3,4-isomer of (dppp)Pt(mannitolate) from 82% to 92%. The present studies further show that very useful empirical observations are readily obtainable, as are key reference data for simple diolate model compounds. Molecular modeling should also prove informative, particularly regarding steric interactions between the phosphine and carbohydrate ligands. It should eventually be possible to enhance the regio- and diastereoselectivities in predictable ways, such as designing chiral auxiliary ligands with strong hydrogen bond acceptor substituents (e.g., amide groups). The ultimate goal is to combine these complexation selectivities with subsequent reaction chemistry at the metal in order to achieve selective transformations of unprotected carbohydrates. Extension to other, more reactive metal systems will be very desirable in this regard. The carbonate–diolate synthesis method developed here may greatly facilitate this, as indicated by recent success in accessing palladium diolate chemistry.[69]

Experimental Section

General. Syntheses and reactions were generally conducted under argon, but synthetic workups can usually be conducted in air if exposure times in solution are limited. Tetrahydrofuran (THF) was distilled under argon from purple sodium benzophenone ketyl. Dichloromethane was distilled under argon from P_2O_5. Pyridine was dried over pellets of potassium hydroxide. Dichloromethane-d_2 was vacuum distilled from calcium hydride. Pyridine-d_5 was dried over activated 4-Å molecular sieves (1/16-in. pellets). Diols and alditols were purchased from Aldrich, Sigma, or Fluka and used as received. Phosphines were purchased from Strem Chemical or Quantum Design. Sodium isopropoxide was prepared by reaction (in toluene) of sodium metal with isopropyl alcohol that had been dried over sodium isopropoxide. Bis(phosphine)platinum(II) dichloride complexes were synthesized from K_2PtCl_4 (***caution: allergen***) according to the procedure of Slack and Baird[70] or from (COD)$PtCl_2$ according to the general procedure of Hackett and Whitesides[71] and were optionally recrystallized by slow diffusion of hexane into a dichloromethane solution to remove traces of water and/or alcohol. All the carbonate complexes can be prepared from the corresponding dichloride and fresh $AgCO_3$, analogous to the literature procedure for (dppe)Pt(CO_3),[33,35] provided that the dichloromethane is wet.[36]

^1H (300 MHz), $^{31}P\{^1H\}$ (121.5 MHz), and ^{13}C and $^{13}C\{^1H\}$ (75.5 MHz) NMR spectra were recorded on a Bruker AM-300 spectrometer at 298 K, except for $^{13}C\{^1H\}$ experiments, which were carried out at 305 K. Pulse widths of ca. 45° were normally employed, with digital resolutions of 0.25 (^1H) and 0.5 Hz (^{31}P and ^{13}C) and acquisition times of 4 (^1H) and 1.8 s (^{31}P and ^{13}C). In several test cases, the integrals obtained for CPD broad-band decoupled ^{31}P spectra were very similar to those obtained under inverse-gated conditions with delays of 35 s. (Typical ^{31}P T_1 values in oxygen-free CD_2Cl_2 at 298 K were 6–8 s for (dppp)Pt diolate, alditolate, and carbonate complexes, while the T_1 for (dcpe)Pt(CO_3) was only 4 s.) Residual solvent resonances were used as internal references for ^1H ($C^1HDCl_2 \equiv \delta$ 5.32) and ^{13}C ($^{13}CD_2Cl_2 \equiv \delta$ 53.8) spectra. 85% H_3PO_4

(62) David, S.; Hanessian, S. *Tetrahedron* **1985**, *41*, 643–663.
(63) Alais, J.; Maranduba, A.; Veyrieres, A. *Tetrahedron Lett.* **1983**, *24*, 2383–2386.
(64) Grindley, T. B.; Thangarasa, R. *J. Am. Chem. Soc.* **1990**, *112*, 1364–1373.
(65) Perlin, A. S. In *The Carbohydrates: Chemistry and Biochemistry*; Pigman, W. W., Horton, D., Eds.; Academic Press: New York, 1980; Vol. IB, pp 1167–1215.
(66) Sklarz, B. *Quart. Rev., Chem Soc.* **1967**, *21*, 3–28.
(67) Foster, A. B. In *The Carbohydrates: Chemistry and Biochemistry*; Pigman, W. W., Horton, D., Eds.; Academic Press: New York, 1972; Vol. 1A, pp 391–396.
(68) Gould, G. L., unpublished results
(69) Koenig, K. S., unpublished results
(70) Slack, D. A.; Baird, M. C. *Inorg. Chim. Acta* **1977**, *24*, 277–280.
(71) Hackett, M.; Whitesides, G. *J. Am. Chem. Soc.* **1988**, *110*, 1449–1462.

(external, δ 0.0) was used as a reference for ^{31}P spectra. NMR multiplicities indicated do not include the 33% abundance ^{195}Pt satellite splittings reported as J_{PtX}. Proton coupling constant assignments were made with the aid of homonuclear decoupling experiments and D_2O exchange of hydroxyl protons. In some cases, only partial proton NMR data are given since extensive peak overlaps occur, especially of minor with major isomers. Elemental analyses were carried out by Schwarzkopf Microanalytical Laboratory, Woodside, NY. Hydrogen analyses for spectroscopically pure compounds tended to be uniformly low, for which no plausible explanation could be deduced.

Synthesis of (dppp)Pt(CO$_3$) via (dppp)Pt(O-*i*-Pr)$_2$. THF (~40 mL) was vacuum transferred from Na/K benzophenone ketyl into a 100-mL Schlenk flask. The flask was taken into a glovebox, and (dppp)PtCl$_2$ (0.689 g, 1.02 mmol) was added to give a white suspension. NaCl (5 mg) was also added to provide seed crystals for the subsequent precipitation to facilitate filtration. Sodium isopropoxide (0.176 g, 2.14 mmol, 2.1 equiv) was then added in aliquots over a period of 5–10 min with stirring. After 3 h, a ^{31}P NMR spectrum of an aliquot showed that formation of (dppp)Pt(O-i-Pr)$_2$ (δ –9.1, s, J_{PtP} = 3163) was complete. The reaction mixture was removed from the glovebox and vacuum filtered through a fine frit into another Schlenk flask to give a pale yellow solution. Water (90 μL, 5 mmol, 5 equiv/Pt) was added to the filtrate, and the stirred solution promptly bubbled with carbon dioxide. Within 1 min, a copious white precipitate formed. The flask was capped under carbon dioxide and allowed to stir for 30 min, after which time the precipitate was isolated by centrifugation, washed in air with ether (3 × 15 mL), and dried under vacuum to give (dppp)Pt(CO$_3$) (0.568 g, 83%). The material was pure by ^{31}P NMR and suitable for most subsequent reactions, but a ^1H NMR showed the presence of ca. 0.1 equiv of ether and 0.05 equiv of THF. When desired, further purification was effected by diffusing hexane (11 mL) into a dichloromethane solution (45 mL) of the complex over a period of 2 days to give a white powder, which was isolated, washed with dichloromethane:hexane (1:1, 3 × 2 mL), and dried under vacuum to give pure product (179 mg, 32% recovery). Further treatment of the mother liquor with hexane gave additional material (303 mg, total recovery of 85%). $^{31}P\{^1H\}$ NMR (CD_2Cl_2): δ –12.0 (s, J_{PtP} = 3377 Hz). IR (Nujol mull): $\nu_{C=O}$ = 1659 cm^{-1}, $2\pi_{CO_3}$ = 1621 cm^{-1}. Anal. Calcd (Found) for $C_{28}H_{26}O_3P_2Pt$: C, 50.37 (50.49); H, 3.93 (3.75).

Typical Synthesis of Diolate Complexes: (dppp)Pt(1,2-ethanediolate). The following preparation is typical. In a glovebox, (dppp)Pt(CO$_3$) (124.5 mg, 186.5 μmol) and 1,2-ethanediol (57.0 mg, 918 μmol, 4.92 equiv) were dissolved in CH_2Cl_2 (15 mL) in a 25-mL screw-capped Erlenmeyer flask. The solution was stirred for 1 h and transferred to a centrifuge tube fitted with a Schlenk adapter top. The tube was taken out of the box and attached to a Schlenk line. The solution was bubbled with Ar for 15 min, stirred a second hour, bubbled with Ar for 15 min, and stirred a third hour. A ^{31}P NMR spectrum of an aliquot taken at that time showed that the reaction was >98% complete. The solvent was removed under vacuum, and the resultant mixture of clear oil and white powder was vacuum dried for 1 h. The powder was washed with deaerated H_2O (3 × 0.5 mL) to remove excess diol, dried under vacuum 4 h, dissolved in a minimum amount of CH_2Cl_2 (2.5 mL), and layered with Et_2O (30.0 mL). Diffusion over 24 h yielded white microcrystals of (dppp)Pt(1,2-ethanediolate) which were washed with Et_2O (3 × 2 mL) and vacuum dried (97 mg, 78%). ***Notes:*** The volume of water used in the wash should be kept to a minimum, since most of the diolate products have some solubility in water. Attempts to drive the reaction to completion using molecular sieves in troublesome cases fostered partial decomposition to the corresponding platinum dichloride complex. ^1H NMR (CD_2Cl_2): δ 7.80 (m, 8 H, Ph), 7.41 (m, 12 H, Ph), 3.57 (t, $|J_{PH} + J_{PH}|$ = 2.6 Hz, J_{PtH} = 31 Hz, 4 H, OCH_2), 2.42 (m, 4 H, PCH_2), 1.95 (br m, 2 H, PCH$_2$CH_2). Anal. Calcd (Found) for $C_{29}H_{30}O_2P_2Pt$: C, 52.18 (52.54); H, 4.53 (4.20).

(dppp)Pt(1,2-propanediolate). Synthesis as for ethanediolate. ^1H NMR (CD_2Cl_2): δ 7.82 (m, 8 H, Ph), 7.40 (m, 12 H, Ph), 3.99 (dddd of q, J_{HH} = 3.8, 6.5 Hz, J_{PH} = 3.8, 0.8 Hz, J_{HCH_3} = 6.0 Hz, J_{PtH} ≈ 30 Hz, 1 H, OCH_ACH$_3$), 3.65 (dddd, J_{HH} = 3.8, 9.2 Hz, J_{PH} = 1.3, 5.4 Hz, J_{PtH} ≈ 38 Hz, 1 H, OCH_BH$_C$), 3.35 (dddd, J_{HH} = 6.5, 9.2 Hz, J_{PH} = 0.9, 3.6 Hz, J_{PtH} ≈ 30 Hz, 1 H, OCH$_B$C), 2.40 (m, 4 H, PCH_2), 1.95 (br m, 2 H, PCH$_2$CH_2), 1.19 (d, J_{HH} = 6.0 Hz, 3 H, CH_3). Anal. Calcd (Found) for $C_{30}H_{32}O_2P_2Pt$: C, 52.86 (53.07); H, 4.73 (4.18).

(dppp)Pt(D-2,3-butanediolate). Synthesis as for ethanediolate. ^1H NMR (CD_2Cl_2): δ 7.88 (m, 8 H, Ph), 7.39 (m, 12 H, Ph), 3.52 (m, 2 H, OCH), 2.38 (br m, 4 H, PCH_2), 1.95 (br m, 2 H, PCH$_2$CH_2), 1.15 (d, J_{HH} = 5.5 Hz, 6 H, CH_3). Anal. Calcd (Found) for $C_{31}H_{34}O_2P_2Pt$: C, 53.52 (53.16); H, 4.93, (5.14).

(dppp)Pt(*meso*-2,3-butanediolate). Synthesis as for ethanediolate. ^1H NMR (CD_2Cl_2): δ 7.9 (m, 8 H, Ph), 7.39 (m, 12 H, Ph), 3.95 (m, 2 H, OCH), 2.4 (br m, 4 H, PCH_2), 1.95 (br m, 2 H, PCH$_2$CH_2), 1.12 (d, J_{HH} = 5.4 Hz, 6 H, CH_3). Anal. Calcd (Found) for $C_{31}H_{34}O_2P_2Pt$: C, 53.52 (53.10); H, 4.93, (5.15).

(dppp)Pt(*trans*-1,2-cyclohexanediolate). Synthesis as for ethanediolate except reaction much slower. ^1H NMR (CD_2Cl_2): δ 7.89 (m, 8 H, Ph), 7.40 (m, 12 H, Ph), 3.27 (~d, J_{HH} ≈ 5 Hz, J_{PH} ≈ J_{PtH} ≈ 0 Hz, 2 H, OCH), 2.37 (br m, 4 H, PCH_2), 1.93 (br m, 2 H, PCH$_2$CH_2), 1.78 (br ~d, 2 H, OCHCH_AH$_B$), 1.47 (br ~d, 2 H, OCHCH$_A$CH_B), 1.20 (br m, 4 H, OCHCH$_2$CH_2). Anal. Calcd (Found) for $C_{33}H_{36}O_2P_2Pt$: C, 54.92 (54.67); H, 5.03 (4.59).

(dppp)Pt(2,3-dimethyl-2,3-butanediolate). Synthesis as for ethanediolate except reaction much slower. ^1H NMR (CD_2Cl_2): δ 7.98 (m, 8 H, Ph), 7.39 (m, 12 H, Ph), 2.35 (m, 4 H, PCH_2), 1.93 (br m, 2 H, PCH$_2$CH_2), 1.24 (s, 12 H, CH_3). Anal. Calcd (Found) for $C_{33}H_{38}O_2P_2Pt$: C, 54.77 (53.60); H, 5.29 (5.23).

(dppp)Pt(phenyl-1,2-ethanediolate). In a glovebox, (dppp)Pt(CO$_3$) (100.7 mg, 150.8 μmol) and phenyl-1,2-ethanediol (90.0 mg, 651.4 μmol, 4.32 equiv) were dissolved in CH_2Cl_2 (10 mL) in a screw-capped Erlenmeyer flask. The solution was stirred for 20 h. The solvent volume was reduced to approximately 5 mL under vacuum, and the pale yellow solution was layered with Et_2O (30.0 mL). The pale yellow waxy crystals of (dppp)Pt(phenyl-1,2-ethanediolate) were isolated, washed with Et_2O (3 × 2 mL), and dried under vacuum to give pure product (78 mg, 70%). ^1H NMR (CD_2Cl_2): δ 7.85 (m, 8 H, Ph), 7.41 (m, 12 + 2 H, Ph), 7.18 (m, 2 H, Ph), 7.09 (m, 1 H, Ph), 4.98 (dd, J_{HH} = 8.9, 4.1 Hz, J_{PH} ≈ J_{PtH} ≈ 0 Hz, 1 H, OCH_APh), 3.78 (ddd, J_{HH} = 9.6, 4.1 Hz, $J_{P(A)H}$ + $J_{P(B)H}$ = 5.8 Hz, J_{PtH} ≈ 65 Hz, 1 H, OCH_BH$_C$), 3.58 (dd, J_{HH} = 9.6, 8.9 Hz, J_{PH} ≈ J_{PtH} ≈ 0 Hz, 1 H, OCH$_B$C), 2.43 (br m, 4 H, PCH_2), 1.99 (br m, 2 H, PCH$_2$CH_2). Anal. Calcd (Found) for $C_{35}H_{34}O_2P_2Pt$: C, 56.53 (56.33); H, 4.61 (4.21).

(dppp)Pt(3-methoxy-1,2-propanediolate). Synthesis as for ethanediolate. ^1H NMR (CD_2Cl_2): δ 7.79 (m, 8 H, Ph), 7.4 (m, 12 H, Ph), 3.8 (m, 2 H), 3.57 (dd, J_{HH} = 9.1, 6.8 Hz), 3.47 (m, 1 H), 3.37 (dd, J_{HH} = 9.1, 5.5 Hz, 1 H), 3.31 (s, 3 H, OCH_3, 2.4 (br m, 4 H, PCH_2), 1.95 (br m, 2 H, PCH$_2$CH_2). Anal. Calcd (Found) for $C_{31}H_{34}O_3P_2Pt$: C, 52.32 (52.04); H, 4.82 (4.47).

(dppp)Pt(glycerolate). In a glovebox, (dppp)Pt(CO$_3$) (100.5 mg, 150.5 μmol) and glycerol (15.4 mg, 167 μmol, 1.1 equiv) were dissolved in CH_2Cl_2 (10 mL) in a screw-capped Erlenmeyer flask. The solution was stirred for 19 h, transferred to a 24/40 diffusion tube, reduced in volume to 5 mL under vacuum, and layered with Et_2O (30 mL). The resulting cream-colored crystals of (dppp)Pt(glycerolate) were isolated and dried under vacuum to give pure product (83 mg, 79%). ^1H NMR (CD_2Cl_2): δ ~7.7 (m, 8 H, Ph), 7.39 (m, 12 H, Ph), 3.86 (dddd, J = 9.8, 4.0, 2.2, ~1 Hz, 1 H, PtOCH_EH$_F$), 3.55 (m, 1 H, PtOCH_D), 3.52 (m, 1 H, CH$_B$CH_COH$_A$), 3.42 (m, 1 H, PtOCH$_B$CH_F), 3.34 (ddd, J = 8.4, 7.9, 2.4 Hz, 1 H, CH_BH$_C$OH$_A$), ~2.5 (br m, 4 H, PCH_2), 2.49 (dd, J = 8.5, 1.6 Hz, 1 H, CH$_2$OH_A), 2.04 (br m, 4 H, PCH_2), 1.82 (br m, 2 H, PCH$_2$CH_2). Anal. Calcd (Found) for $C_{30}H_{32}O_3P_2Pt$: C, 51.65 (51.36); H, 4.62 (4.20).

(dppp)Pt(1,2,4-butanetriolate). In a glovebox, (dppp)Pt(CO$_3$) (203.8 mg, 305.3 μmol) and 1,2,4-butanetriol (33.9 mg, 319 μmol, 1.05 equiv) were dissolved in CH_2Cl_2 (20 mL) in a screw-capped Erlenmeyer flask. The solution was stirred for 2 h, transferred to a centrifuge tube fitted with a Schlenk adapter top, and purged with argon four times over another 3 h. A ^{31}P NMR spectrum of an aliquot showed that the reaction was >95% complete. The solvent was removed under vacuum, and the resulting white powder was dried under vacuum 1 h, dissolved in a minimum amount of CH_2Cl_2 (1.25 mL), and layered with ether (10 mL). The resulting crystals of (dppp)Pt(1,2,4-butanetriolate) were isolated and dried under vacuum (190 mg, 87%). ^1H NMR (CD_2Cl_2): δ 7.74 (m, 6 H, Ph), 7.63 (m, 2 H, Ph), 7.41 (m, 12 H, Ph), 5.15 (dd, J_{HH} = 7.6, ~1 Hz, 1 H, CH$_2$OH_A), 4.04 (br m, J_{PtH} ≈ 0, 1 H, PtOCH_F), 3.67 (ddt, J_{HH} = 3.5, ~1, 10.3 Hz, 1 H, CH_BH$_C$OH), ~3.5 (m, 3 H, CH$_B$CH_COH, PtOCH_GH$_H$), 2.4 (m, 4 H, PCH_2), 1.9 (m, 2 H, PCH$_2$CH_2), 1.6 (m, 2 H, CH_DH$_E$-CH$_2$OH). Homonuclear decoupling shows that H_A is coupled to H_B, which is in turn coupled to $H_{D/E}$, with coupling constants of 10.3 and 3.5 Hz, identifying the complex as the 1,2-bound isomer. The 2,4-bound isomer would not be expected to have significant coupling between H_B and $H_{D/E}$. Anal. Calcd (Found) for $C_{31}H_{34}O_3P_2Pt$: C, 52.32 (51.84); H, 4.82 (4.19).

Typical Synthesis of Alditolate Complexes: (dppp)Pt(erythritolate). The following preparation is typical. In a glovebox, (dppp)Pt(CO$_3$) (101.4 mg, 152 μmol) and erythritol (74.2 mg, 608 μmol, 4 equiv) were loaded into a 25-mL Schlenk flask. The flask was taken out of the box and

attached to a Schlenk line. The solids were dissolved in pyridine (15 mL), and the solution was stirred for 22 h with periodic argon purges. At that time, a ^{31}P NMR spectrum of an aliquot showed that the reaction was >98% complete. The solvent was removed under vacuum, and the resulting mixture of white powder and clear oil was vacuum dried for 3 h. The product was extracted into CH_2Cl_2 (20 mL) and separated from the undissolved excess erythritol by centrifugation. The solution was transferred to a 24/40 diffusion tube, reduced in volume to 5 mL under vacuum, and layered with Et_2O (30 mL). Diffusion over 24 h yielded white block crystals of (dppp)Pt(erythritolate) which were vacuum dried (73 mg, 66%). Anal. Calcd (Found) for $C_{31}H_{34}O_4P_2Pt\cdot CH_2Cl_2$: C, 47.30 (47.65); H, 4.47 (4.12).

(dppp)Pt(1,2-erythritolate). ^1H NMR (CD_2Cl_2): δ 7.79 (m, 4 H, Ph), 7.40 (m, 16 H, Ph), 6.19 (dd, J_{HH} = 3.1, 10.7 Hz, 1 H, $CH_CH_BOH_A$), 4.02 (ddd, J_{HH} = 3.1, 11.1, 9.7 Hz, 1 H, $CH_CH_BOH_A$), 3.93 (dd, J_{HH} = 5.3, 10.3 Hz, J_{PH} = ~1, ~1 Hz, 1 H, OCH_GH_H (ax)), 3.53 (dddd, J_{HH} = 1.9, 10.3 Hz, J_{PH} = 1.9, 7.2 Hz, J_{PtH} ≈ 60 Hz, 1 H, OCH_GH_H (eq)), 3.43 (m, J_{HH} = 3.5, 5.3, ~1.9 Hz, J_{PH} = 7.2, ~1.9 Hz, J_{PtH} = ~50 Hz, 1 H, $OCH_FCH_EOH_D$ (eq)), 3.29 (ddd, J_{HH} = 10.7, 11.1, 4.4 Hz, 1 H, $CH_CH_BOH_A$), 3.15 (dddd, J_{HH} = 9.7, 4.3, 9.9, 3.5 Hz, 1 H, $OCH_FCH_EOH_D$), 1.89 (d, J_{HH} = 9.9 Hz, 1 H, $OCH_FCH_EOH_D$), ~2.69, ~2.38, ~2.17, ~1.64 (br, m, 6 H, $PCH_2CH_2CH_2P$).

(dppp)Pt(2,3-erythritolate). ^1H NMR (CD_2Cl_2): (partial) δ ~3.40 (m, J = ~10.0, ~4.1, ~3.5 Hz, CH_2), 2.53 (dd, J = 6.8, 4.0 Hz, OH). **(dppp)Pt(DL-threitolate).** Synthesis as for erythritolate. Anal. Calcd (Found) for $C_{31}H_{34}O_4P_2Pt$: C, 51.17 (50.91); H, 4.71 (4.77).

(dppp)Pt(2,3-DL-threitolate). ^1H NMR (CD_2Cl_2): δ 7.79 (m, 4 H, Ph), 7.65 (m, 4 H, Ph), 7.41 (m, 12 H, Ph), ~3.9–3.2 (several m, 6 H, CH's), ~2.48 (br, m, 4 H, PCH_2), 2.47 (dd, J = 9.2, 1.2 Hz, 2 H, OH), 1.94 (br m, 2 H, PCH_2CH_2).

(dppp)Pt(1,2-DL-threitolate). ^1H NMR (CD_2Cl_2): (partial) δ 4.27 (dd, J = 6.1, 1.2 Hz, 1 H, OH), 3.29 (d, J = 3.7 Hz, 1 H, OH).

(dppp)Pt(ribitolate). Synthesis as for erythritolate. Anal. Calcd (Found) for $C_{32}H_{36}O_5P_2Pt\cdot 0.5(C_2H_5)_2O$: C, 51.38 (51.47); H, 5.20 (5.41).

(dppp)Pt(1,2-ribitolate). ^1H NMR (CD_2Cl_2): (partial) δ 7.19 (d, J = 2.3 Hz, 1 H, CHOH), 4.2 (m, 1 H), 3.95 (dd, J = 10.6, 5.3 Hz, 1 H), 3.75 (m, 1 H), 3.55 (m, 2 H), 3.35 (m, 1 H), 3.00 (dd, J = 6.4, 5.7 Hz, 1 H, CH_2OH), 2.93 (dt, J = 3.9, 9.4 Hz, 1 H), 2.08 (d, J = 9.8 Hz, 1 H, CHOH).

(dppp)Pt(2,3-ribitolate). ^1H NMR (CD_2Cl_2): (partial) δ 4.86 (dd, J = 9.6, 4.5 Hz, 1 H, CH_2OH).

(dppp)Pt(xylitolate). Synthesis as for erythritolate. Anal. Calcd (Found) for $C_{32}H_{36}O_5P_2Pt\cdot 0.25(C_2H_5)_2O$: C, 51.06 (50.72); H, 5.00 (5.12).

(dppp)Pt(2,3-xylitolate). ^1H NMR (CD_2Cl_2): (partial) δ 2.29 (dd, J = 8.8, 1.5 Hz, 1 H, CH_2OH).

(dppp)Pt(galactitolate). Synthesis as for erythritolate. Anal. Calcd (Found) for $C_{33}H_{38}O_6P_2Pt$: C, 50.32 (49.69); H, 4.86 (5.04).

(dppp)Pt(2,3-galactitolate). ^1H NMR (CD_2Cl_2): (partial) δ 4.37 (d, J = 4.1 Hz, 1 H, CHOH).

(dppp)Pt(D-mannitolate). Synthesis as for erythritolate. Anal. Calcd (Found) for $C_{33}H_{38}O_6P_2Pt\cdot CH_2Cl_2$: C, 46.80 (46.81); H, 4.62 (4.36).

(dppp)Pt(3,4-D-mannitolate). ^1H NMR (CD_2Cl_2): δ 7.59 (m, 4 H, Ph), 7.42 (m, 16 H, Ph), 5.11 (dd, J_{HH} = 3.5, 9.7 Hz, 2 H, $CH_CH_BOH_A$), 4.00 (ddd, J_{HH} = 3.6, 11, 8.7 Hz, 2 H, $CH_CH_BOH_A$), 3.57 (m, J_{HH} = 4.5 Hz, J_{PH} = 5.0 Hz, J_{PtH} ≈ 58 Hz, 2 H, OCH_F (eq)), 3.44 (ddd, J_{HH} = 9.8, 11, 4.6 Hz, 2 H, $CH_CH_BOH_A$), 3.33 (dddd, J_{HH} = 8.7, 4.6, 8.8, 4.5 Hz, 2 H, CH_EOH_D), 2.59 (br m, 4 H, PCH_2), 2.19 (d, J_{HH} = 8.8, 2 H, CH_EOH_D), 2.00 (br m, 2 H, PCH_2CH_2).

(dppp)Pt(2,3-D-mannitolate). ^1H NMR (CD_2Cl_2): (partial) δ 4.84 (dd, J_{HH} = 4.2, 9.8 Hz, 1H, OH), 2.85 (d, J_{HH} = 8.9 Hz, 1H, OH), 2.41 (d, J_{HH} = 9.6 Hz, 1H, OH), 2.19 (dd, J_{HH} = 7.9, 3.4 Hz, 1H, OH).

Measurement of Relative Diol Complexation Constants. A. Typical Phosphine Competition Reaction. In the glovebox, (dppp)Pt(CO_3) (3.5 mg, 5.2 μmol), (dtpe)Pt(CO_3) (3.5 mg, 4.9 μmol), and (dppv)Pt(CO_3) (3.4 mg, 5.2 μmol) were dissolved in CH_2Cl_2 (0.5 mL) in a screw-capped NMR tube. A 0.284 M stock solution of 1,2-ethanediol (ED) was prepared in a 5 mL volumetric flask by dissolving ED (88.1 mg, 1.42 mmol) in CH_2Cl_2 and diluting to the mark. An aliquot of the stock solution (216 μL, 4 equiv ED based on total Pt(CO_3)) was then added to the NMR tube. The reaction was monitored by ^{31}P NMR, the final spectrum being run with inverse-gated decoupling. The percent conversion to diolate complex for the three carbonates at the given times were (dppp, dtpe, dppv): 38, 65, 93 at 0.5 h; 38, 66, 93 at 6 h; 39, 67, 93 at 24 h; and 39, 66, 93 at 36 h. The complexation constant K_{dppp} = [(dppp)Pt(ED)][H_2O][CO_2]/[(dppp)Pt(CO_3)][ED]. K_{dppp}/K_{dtpe} is then equal to [(dppp)Pt(ED)][(dtpe)Pt(CO_3)]/[(dppp)Pt(ED)][(dtpe)Pt(CO_3)] (since [H_2O], [CO_2], and [ED] cancel out in the ratio of K's). Substituting in the observed percent compositions, which are directly proportional to the concentrations, and setting $K_{dppp} \equiv 1$, gives $K_{dppp}:K_{dtpe}:K_{dppv}$ = 1:3.0:22, 1:3.2:22, 1:3.3:21, 1:3.0:21 at the four times, respectively.

B. Phosphine Competition Reactions with Pinacol. In the glovebox, (dppe)Pt(CO_3) (3.0 mg, 4.6 μmol), (dppp)Pt(CO_3) (3.1 mg, 4.6 μmol), (dcpe)Pt(CO_3) (3.2 mg, 4.7 μmol), and pinacol (11.0 mg, 93 μmol, 6.7 equiv based on total Pt(CO_3)) were dissolved in CD_2Cl_2 to give a total reaction volume of 0.59 mL. The reaction was monitored by ^{31}P NMR over a period of 4 days, at which time equilibrium had been reached, with the percent conversion to diolate complex for the three carbonates 89% (dppe), 52% (dppp), and 1% (dcpe). Setting $K_{dppe} \equiv 1000$, gives $K_{dppe}:K_{dppp}:K_{dcpe}$ = 1000:100:1. In a reverse experiment, (dcpe)Pt(pin) (4.6 mg, 6.3 μmol), (dppp)Pt(CO_3) (4.1 mg, 6.1 μmol), and pinacol (13.1 mg, 111 μmol) were dissolved in CD_2Cl_2 to give a total reaction volume of 0.5 mL. The reaction was monitored by ^{31}P NMR over a period of 4 days, at which time equilibrium had been reached ((dppp)Pt(pin):(dppp)Pt(CO_3):(dcpe)Pt(pin):(dcpe)Pt(CO_3) = 5.13:0.36:0.82:6.09), again giving $K_{dppp}:K_{dcpe}$ = 100:1. The values of $K_{dppp}:K_{dcpe}$ for the last two spectra of the two experiments were 93, 106, 127, and 106, for an average of 108 ± 12.

C. Typical Diol Competition Reaction. A 1.0-mL stock solution of *cis*-1,2-cyclohexanediol (CHD, 7.3 mg, 63 μmol) and D-2,3-butanediol (BD, 5.5 mg, 61 μmol) in dichloromethane was prepared in a 1.0-mL volumetric flask in the glovebox. A 500-μL aliquot was added to (dppp)Pt(CO_3) (10.0 mg, 15.0 μmol) in a screw-capped NMR tube (*cis*-1,2-cyclohexanediol = 2.1 equiv, D-2,3-butanediol = 2.0 equiv) and mixed. The reaction was then monitored by ^{31}P NMR, which gave essentially identical results at 3, 5, and 9.5 h: (dppp)Pt(*cis*-1,2-cyclohexanediolate):(dppp)Pt(D-2,3-butanediolate):(dppp)Pt(CO_3) = 26:25:49. From this, K_{CHD}/K_{BD} = [(dppp)Pt(CHD)][BD]/[(dppp)Pt(BD)][CHD] = (0.26)(2.0 – 0.25)/(0.25)(2.1 – 0.26) = 0.99.

D. Typical Diol/Diolate Competition Reaction. The complex (dppp)Pt(1,2-ethanediolate) (10.2 mg, 15.3 μmol) was dissolved in CD_2Cl_2 (0.48 mL) in a screw-capped NMR tube, and a 50-μL aliquot (15 μmol, 0.99 equiv) of a stock solution of 1,2-propanediol (PD, 23.0 mg, 302 μmol in 1.0 mL of CH_2Cl_2) was added. The reaction was then monitored by ^{31}P NMR at 7-min intervals, which showed partial conversion of (dppp)Pt(1,2-ethanediolate) to (dppp)Pt(1,2-propanediolate). An equilibrium distribution of 52:48 ethanediolate:propanediolate was reached after 1–3 h. From this, K_{PD}/K_{ED} = [(dppp)Pt(PD)][ED]/[(dppp)Pt(ED)][PD] = (0.48)(0.48)/(0.52)(0.99 – 0.48) = 0.87. In a direct competition between 1,2-ethanediol, 1,2-propanediol, and pinacol with (dppp)Pt(CO_3), K_{PD}/K_{ED} was determined to be 0.72.

E. 1,2- vs 1,3-Diol Complexation. Pinacol (19.3 mg, 163 μmol) and 2,2-dimethyl-1,3-propanediol (DMPD, 150.7 mg, 1447 μmol) were dissolved in dichloromethane and diluted to the mark in a 2.0-mL volumetric flask. A 200-μL aliquot of this stock solution was added to a solution of (dppp)Pt(CO_3) (5.0 mg, 7.5 μmol) in CD_2Cl_2 (350 μL) in a screw-capped NMR tube (pinacol = 2.2 equiv, DMPD = 19.3 equiv). The reaction was then monitored by ^{31}P NMR, which gave (dppp)Pt(CO_3):(dppp)Pt(pinacolate):(dppp)Pt(2,2-dimethyl-1,3-propanediolate) ratios of 91.1:1.7:7.2 at 0.5 h, 78.5:13.9:7.6 at 4.5 h, 70.2:26.2:3.6 at 24 h, 72.3:24.7:3.0 at 48 h, 73.7:23.8:2.5 at 72 h, and 74.1:22.7:3.3 at 5 days. Derived values for K_{Pin}/K_{DMPD} at the above times were 2, 17, 73, 84, 96, and 69, giving an average K_{rel} = 81 ± 11 for the last four equilibrium points. Under these conditions of excess diol, the ^{31}P chemical shifts and ^{195}P–^{31}P coupling constants for the three complexes were –11.9 (3409 Hz), –9.1 (3181 Hz), and –7.0 (3239 Hz), respectively.

X-ray Structure Determination of (dppp)Pt(3,4-D-mannitolate)·CH_2Cl_2. Crystals of (dppp)Pt(3,4-D-mannitolate)·CH_2Cl_2 were obtained by carefully layering a dichloromethane solution of the complex with ether and setting it aside to permit slow diffusion to occur. The colorless crystal selected for the experiment had dimensions 0.4 × 0.4 × 0.4 mm and exhibited the forms {100} and {011}. X-ray data were collected at room temperature using an Enraf-Nonius CAD4 diffractometer with graphite-monochromatized Mo Kα radiation (λ = 0.7107 Å). From the systematic absences, the space group was determined to be $P2_12_12_1$. The cell parameters (a = 11.225(2) Å, b = 15.875(3) Å, c = 19.964(4) Å) were obtained by a least-squares fit of $\sin^2\theta$ values for 25 reflections in the range 9° < θ < 10°, each of which was measured at two equivalent positions (one with positive and one with negative θ). Integrated intensities were measured by ω/2θ scans with ω-scan width (1.00 + 0.35 tan θ), using varying scan speeds determined by a prescan. Three standard reflections (019, 165, 523) were monitored every 60 min. The measured

intensities were subsequently scaled to compensate for the ca. 8% loss in intensity of the standard reflections that occurred during the data collection. An octant of data ($\theta < 30°$; $h \leq 15$, $k \leq 22$, $l \leq 28$) was collected, yielding a total of 5772 measured reflections, excluding standard reflections, 4034 having $F_o > 3\sigma(F_o)$. Lorentz, polarization, and analytical absorption[72] corrections were applied, absorption coefficient $\mu = 44.4$ cm^{-1}, which gave correction factors in the range 0.423–0.529.

A partial starting structure was found using direct methods.[73] All remaining atoms were found in successive difference maps after refinements by differential Fourier methods.[74] The positional and isotropic displacement parameters so obtained were then used as starting input to a full-matrix least-squares refinement utilizing the program POP.[75] Using the 4034 reflections with $F_o > 3\sigma(F_o)$, 407 parameters were varied, including the positional and anisotropic displacement parameters of the non-hydrogen atoms, together with the scale factor and isotropic extinction parameter g for a type I crystal with Lorentzian mosaicity.[76] The quantity minimized was $\sum w||F_o| - |F_c||^2$ with weights $w = 1/\sigma^2(F_o)$ and $\sigma^2(F_o) = \sigma_{cs}^2 + (0.02\ F_o)^2$, where σ_{cs}^2 is the variance due to counting statistics. Atomic scattering factors were those as calculated by Cromer and Waber.[77] Anomalous dispersion corrections were included for all atoms.[78] The refinement converged ($\Delta/\sigma < 0.01$) with fit indices $R(F_o) = 0.058$, $R_w(F_o) = 0.062$, and $S = 1.91$, isotropic extinction parameter $g = 0.63(18)$, where $R = \sum||F_o| - |F_c||/\sum|F_o|$, $R_w = (\sum w(|F_o| - |F_c|)^2/\sum w|F_o|^2)^{1/2}$, and $S = (\sum w(|F_o| - |F_c|)^2/(N_o - N_v))^{1/2}$, where N_o is the number of observed reflections (4034) and N_v is the number of variables (407).

Atomic coordinates and anisotropic displacement parameters are listed in Table S-I. Selected distances and angles are given in Tables 5 and 6, with full listings given in Tables S-II and S-III. Observed and calculated structure factor amplitudes are given in Table S-IV.

Acknowledgment. The authors would like to thank undergraduate researchers Kristina Koenig, Nicole Brunkan, and Michael George (supported under the U.S. Department of Energy's Office of University and Science Education Programs, Office of Energy Research) for carrying out a few of the experiments reported here and Drs. Kathi Barkigia, Richard McMullan, and Morris Bullock for helpful discussions. This research was carried out at Brookhaven National Laboratory under contract DE-AC02-76CH00016 with the U.S. Department of Energy and was supported by its Division of Chemical Sciences, Office of Basic Energy Sciences.

Supplementary Material Available: Additional NMR spectroscopic data, Figures S-1 and S-2; and tables of X-ray crystal structure atomic coordinates, thermal parameters, distances, and angles, (7 pages); listing of observed and calculated structure factors (35 pages). This material is contained in many libraries on microfiche, immediately follows this article in the microfilm version of the journal, and can be ordered from the ACS; see any current masthead page for ordering information.

(72) Busing, W. R.; Levy, H. A. *Acta Crystallogr.* **1957**, *10*, 180–182.
(73) Gilmore, G. J. *MITHRIL. A Computer Program for the Automatic Solution of Crystal Structures from X-ray Data;* Department of Chemistry, University of Glasgow: Glasgow, Scotland, 1983.
(74) Sheldrick, G. M. *SHELX-76, Program for Crystal Structure Determination*; University of Cambridge: Cambridge, England, 1976.
(75) Craven, B. M.; Weber, H. P.; He, X. M. *The POP Least-Squares Refinement Procedure*; University of Pittsburgh: Pittsburgh, PA, 1987.
(76) Becker, P. J.; Coppens, P. *Acta Crystallogr.* **1974**, *A30*, 129–147.
(77) Cromer, D. T.; Waber, J. T. *International Tables for X-ray Crystallography;* Kynoch Press: Birmingham, England, 1974; Vol. IV, pp 71–147.
(78) Cromer, D. T.; Ibers, J. A. *International Tables for X-ray Crystallography;* Kynoch Press: Birmingham, England, 1974; Vol. IV, pp 148–151.